Leptin Signalling in the Ovary of Diet-Induced Obese Mice Regulates Activation of Nod-Like Receptor Protein 3 Inflammasome

Marek Adamowski[1], Karolina Wołodko[1], Joana Oliveira[2], Juan Castillo-Fernandez[3], Daniel Murta[4,5], Gavin Kelsey[3,6], António M. Galvão[1,3,6*]

[1]Department of Reproductive Immunology and Pathology, Institute of Animal Reproduction and Food Research of Polish Academy of Sciences, Olsztyn, Poland

[2]Centro de Investigação em Ciências Veterinárias, Lusófona University , Lisbon, Portugal

[3]Epigenetics Programme, The Babraham Institute, Cambridge, CB22 3AT, UK

[4]Centro de Investigação Interdisciplinar Egas Moniz (CiiEM), Escola Superior de Saúde Egas Moniz, Campus Universitário, Quinta da Granja, Monte de Caparica, Portugal

[5]C.I.I.S.A., Faculty of Veterinary Medicine, University of Lisbon, Lisbon, Portugal

[6]Centre for Trophoblast Research, University of Cambridge, Cambridge, CB2 3EG, UK

*** Correspondence:**
António M. Galvão
antonio.galvao@babraham.ac.uk

Keywords: ovary, inflammation, leptin, obesity, NLRP3inflammasome

1 Abstract

Obesity leads to ovarian dysfunction and the establishment of local leptin resistance. The aim of our study was to characterise levels of Nod-Like Receptor Protein 3 (NLRP3) inflammasome activation during obesity progression in the mouse ovaries and liver and test the putative role of leptin on its regulation. C57BL/6J mice were treated with equine chorionic gonadotropin (eCG) or human chorionic gonadotropin (hCG) for oestrous cycle synchronisation and ovaries collection. In diet-induced obesity (DIO) model, mice were fed chow diet (CD) or high fat diet (HFD) for 4 or 16 weeks (wk), whereas in hyperleptinemic model (LEPT), mice were injected with leptin for 16 days (16L) or saline (16C) and in the genetic obese leptin-deficient *ob/ob* (+/? and -/-) animals were fed CD for 4wk. Either ovaries and liver were collected, as well as cumulus cells (CCs) after superovulation from DIO and LEPT. In DIO protocol, protein expression of NLRP3 inflammasome components was increased in 4wk HFD, but decreased in 16wk HFD. Moreover LEPT and *ob/ob* models revealed NLRP3 and IL-1β upregulation in 16L and downregulation in *ob/ob*. Transcriptome analysis of CC showed common genes between LEPT and 4wk HFD modulating NLRP3 inflammasome. Moreover analysis in the liver showed upregulation of NLRP3 protein only after 16wk HFD, but also the downregulation of NLRP3 protein in *ob/ob*-/-. We showed the link between leptin signalling and NLRP3 inflammasome activation in the ovary throughout obesity progression in mice, elucidating the molecular mechanisms underpinning ovarian failure in maternal obesity.

2 Introduction

Obesity leads to self-directed tissue inflammation, a process mostly promoted by the continuous expansion of adipose tissue (Hotamisligil and Erbay 2008; Odegaard and Chawla 2008). Furthermore, literature presents a solid link between obesity and reproductive failure in women (Chu et al. 2007). Indeed, obesity in women has been associated to ovarian dysfunction, embryo implantation failure, abortion, foetal congenital abnormalities, and adult offspring adiposity and metabolic dysfunction (Chu et al. 2007; Penzias 2012; Robker 2008; Samuelsson et al. 2008). The ovaries from mice fed high fat diet (HFD) showed increased apoptosis and fewer mature oocytes (Jungheim et al. 2010). Furthermore, due to lipid accumulation, endoplasmic reticulum (ER) stress, mitochondrial dysfunction and increased ovarian cell apoptosis, these mice displayed anovulation and reduced *in vivo* fertilization rates (Wu et al. 2010), as well as abnormal embryo development (Minge et al. 2008). We have recently demonstrated the establishment of leptin resistance in the ovaries of mice treated with HFD (Wołodko et al. 2020) was mostly mediated by suppressor of cytokine signalling 3 (SOCS3). Hence, changes in local leptin signalling were shown to contribute to the pathophysiology of ovarian failure in obese females (Wołodko et al. 2021).

The inflammasome is a large intracellular protein complex that contains a cytosolic pattern recognition receptor. Among NOD-like receptors (NLR), the NLR protein 3 (NLRP3) inflammasome has been best characterised as a complex of proteins responsible for controlling the activity of two proinflammatory cytokines interleukin (IL)-1β and IL-18 (Davis, Wen, and Ting 2011; De Nardo and Latz 2011; Martinon, Burns, and Tschopp 2002). Activation of the pattern recognition receptor NLRP3 can be accomplished through two major signals: (i) priming signal, induced by the toll-like receptor (TLR)/nuclear factor (NF)-κB pathway; and (ii) pathogen-associated molecular patterns (PAMPs) and damage-associated molecular patterns (DAMPs) leading to assembly of inflammasome

(Lamkanfi and Dixit 2014; Martinon, Burns, and Tschopp 2002). Both mechanisms lead to the recruitment of the adapter apoptosis-associated speck-like protein containing a C-terminal caspase recruitment domain (ASC), resulting in the activation of pro-caspase-1 (CASP1) and cleavage into the active form (Davis, Wen, and Ting 2011). The formation and activation of the inflammasome is possible through ASC, which links NLRP3 to CASP1 by means of its pyrin and caspase recruitment domain motifs (Martinon et al. 2006). Finally, activated CASP1 is known to process the maturation of IL-1β and IL-18 into active cytokines (Lamkanfi 2011). Importantly, obesity and insulin resistance (IR) have been associated with inflammation and subsequent activation of NLRP3 inflammasome (Traba and Sack 2017). The onset of inflammasome activation was also shown to be mediated by factors like glucose, ceramide, uric acid, or lipopolysaccharide (LPS) (Stienstra et al. 2012; Traba and Sack 2017). Furthermore, secondary signals could also come from extracellular ATP inducing K+ efflux; DAMPs/PAMPS leading to reactive oxygen species (ROS) production (Shao et al. 2015; Tőzsér and Benkő 2016). Saturated free fatty acids (FFAs) were equally linked to inflammasome activation through both signals (Wen et al. 2011), as increased levels of FFAs are a general feature of obesity, IR or type-2 diabetes (Boden 2002; Krebs and Roden 2005). More recently, a link has been also established between NLRP3 inflammasome activation and levels of leptin signalling in various cellular contexts (Fu et al. 2017), corroborating the proinflammatory role of leptin (Cauble et al. 2018).

A recent report has shown the presence of NLRP3 inflammasome components at ovarian level during follicular development in mice, suggesting its involvement in ovulation (Z. Zhang, Wang, and Zhang 2019). Most importantly, NLRP3 was also suggested to be involved in the pathophysiology of polycystic ovary syndrome (PCOS) (Rostamtabar et al. 2020). Therefore, we presently hypothesise the regulation of NLRP3 in the ovary of obese mice is mediated by leptin signalling. We firstly confirmed NLRP3 inflammasome expression profile changed in the ovaries of

cyclic mice. Subsequently, we also confirmed NLRP3 inflammasome components were differently expressed in the ovaries of 4 and 16 weeks (wk) diet induced obese (DIO) mice. Furthermore, using a mouse model of pharmacological hyperleptinemia (LEPT) and a genetic obese mouse which lacks leptin (*ob/ob*) we demonstrated the association between levels of leptin signalling and NLRP3 inflammasome activation in the ovary of obese mice. Moreover, we analysed the transcriptome of cumulus cells (CCs), the somatic companions of the oocyte, and concluded once more that leptin treatment-upregulated genes associated with NLRP3 inflammasome. Finally, we studied the NLRP3 inflammasome expression in the liver of DIO, LEPT and *ob/ob* mice and despite observing a different temporal signature in DIO, with regard to the ovary, we also found a consistent downregulation in NLRP3 inflammasome activity in *ob/ob*, which are obese and lack leptin.

3 Materials & Methods

3.1 Animals

Female B6 mice (8 wk old) and B6.Cg-Lepob/J (*ob/ob*) were housed in the Animal Facility of Institute of Animal Reproduction and Food Research, Polish Academy of Sciences in Olsztyn. Breeding pairs were purchased from Jackson Laboratories (Bar Harbor, ME). Mice were housed with free access to food and water for the duration of the study (humidity 50±10%; 23^{o}C; 12L:12D cycle). All procedures were approved by the Local Animal Care and Use Committee for University of Warmia and Mazury, Olsztyn. Guidelines for animal experiments followed EU Directive 2010/63/EU. Throughout the whole experiments, mice were monitored for any sings of welfare or disease. At 21 days of age female progeny were weaned and housed in groups of 3–5 in plastic cages with fresh sawdust bedding. By 8 wk of age, one group of B6 mice was subjected to hormonal protocol, while the other group was segregated into two different dietary protocols matched for similar body weight. In DIO model (n=10/group) mice were placed on standard CD (Picolab Rodent

125 diet 20, #5053) with 13% of calories coming from fat, or on HFD with 59 % of calories coming from
126 fat (AIN-76A with 33% hydrogenated coconut oil; LabDiet) for 4 or 16 wk. Hyperleptinemia model
127 (n=8/group) was utilized to mimic high level of leptin through its intraperitoneal injections twice a
128 day at total dosage 100 µg/day (injected at 09:00 and 21:00), while the control group received saline
129 injections(Recombinant Mouse Leptin, GFM26, Cell Guidance Systems). Regarding *ob/ob* model
130 (n=6/group), mice were kept on CD until 12 wk of age.

131 *3.2 Induction of oestrus and dioestrus stages*

132 The oestrous cycle was monitored studying vaginal cytology. Cells collected via saline lavage
133 were placed on glass slide and stained with Diff Quik® kit (Medion Diagnostics AG, Switzerland,
134 DQ-ST). Oestrus was characterised by cornified epithelium cells; metoestrus by both cornified cells
135 and leukocytes; dioestrus by predominant leukocytes; and pro-oestrus by nucleated cells, as
136 previously described (Kyrönlahti et al. 2011).

137 Group of female B6 mice (8 wk old) was injected in oestrus stage with eCG (G4877, 5IU, Sigma
138 Aldrich, Saint Louis, Missouri, USA) followed after 48 h by hCG (Chorulon, 5IU, MSD Animal
139 Health, Boxmeer, Netherlands) and tissues collected 18-20 h later in E. The second group of mice
140 were injected with hCG and tissues were collected 16-18 h later in D. To reduce variation between
141 groups ovaries from females from the remaining experiments were collected in dioestrus stage.

142 *3.3 Protein extraction and Western blotting analysis*

143 Protein expression in mouse ovary and liver was assessed by Western blotting. Ovaries and livers
144 were homogenized with RIPA buffer (R0278; Sigma) containing protease inhibitors
145 (phenylmethylsulfonyl fluoride, PMSF and Protease Inhibitor Cocktail, P8340; Sigma-Aldrich, St.
146 Louis, MO, US) and phosphatase inhibitors (Pierce Phosphatase Inhibitor Mini Tablets 88667;

Thermo Fisher Scientific) and incubated on ice for 1 h while vortexing in the meantime. After centrifugation (20 000 g, 15 min, 4°C) the supernatants were collected and protein concentration was determined with the Smith (Smith 1985) copper/bicinchoninic assay (Copper (II) Sulfate, C2284; Sigma and Bicinchoninic Acid Solution, B9643, Sigma). Samples were run (40 µg of protein) on 10-18% polyacrylamide gels. Immunoblotting was performed using the following primary antibodies NLRP3 (AG-20B-0014-C100; Adipogen), CASP1 (ab108362; Abcam), IL-18 (ab71495; Abcam), β-actin (A2228; Sigma), glyceraldehyde 3-phosphate dehydrogenase (GAPDH, ab9485; Abcam) and then transferred to nitrocellulose (10600009; GE Healthcare Life Science) or polyvinylidene fluoride (PVDF) membrane (IPVH00010; Merck Millipore). The membranes were blocked in phosphatase buffered saline (PBS) solution containing 3% powdered milk for 1 h. Primary antibodies were used at 1:1 000 (NLRP3, CASP1) and 1:250 (IL-18) dilution and incubated overnight at 4°C. The following day, proteins were detected by incubating the membranes with a polyclonal anti-mouse horseradish peroxidase (HRP)-conjugated secondary (1:10 000, 31430; Thermo Fisher Scientific), polyclonal anti-rabbit HRP-conjugated secondary (1:20 000, 31460; Thermo Fisher Scientific), polyclonal anti-mouse alkaline phosphatase-conjugated secondary (1:10 000, 31321; Thermo Fisher Scientific) and polyclonal anti-rabbit alkaline phosphatase-conjugated secondary (1:10 000, A3687, Sigma) antibodies, for 1,5 h in chemiluminescence method or 2,5 h in colorimetric method at room temperature (RT). All antibodies specifications are summarised in **Table 1**. Immunocomplexes were visualized subsequently using chemiluminescence detection reagent (SuperSignal West Femto kit, 34095; Thermo Fisher Scientific) or chromogenic substrate NBT/BCIP diluted 1:50 (11681451001; Roche) in alkaline phosphate buffer. Band density for each of the target protein was normalised against β-actin for NLRP3 and IL-18, while GAPDH was used for CASP1 as a reference protein. Finally, bands were quantified using the ChemiDoc or VersaDoc MP 4000 imaging system (Bio-Rad). Quantitative measurements of blot intensity were performed using ImageLab software.

3.4 Total RNA Isolation and cDNA Synthesis

Total RNA was extracted from whole ovary and 10 mg of liver, using TRI reagent (T9424; Sigma Aldrich) following the manufacturer's instructions. RNA samples were stored at -80^{o}C. Concentration and quality of RNA was determined spectrophotometrically and the ratio of absorbance at 260 and 280 ($A_{260/280}$) was analysed confirming good RNA quality. Subsequently, 2 µg of RNA was reverse transcribed into cDNA using Maxima First Strand cDNA Synthesis Kit for RT-qPCR (K1642; ThermoFisher Scientific) (Galvão et al. 2012).

3.5 Real-time PCR

Real-time PCR assays were performed in a 7900 Real-time System (Applied Biosystems), using a default thermocycler program for all genes: a 10 min preincubation at 95°C was followed by 45 cycles of 15 sec at 95°C and 1 min at 60°C. A further dissociation step (15 sec at 95°C, 15 sec at 60°C, and 15 sec at 95°C) ensured the presence of a single product. *Ribosomal protein L37 (Rpl37)* was chosen as a house keeping gene and quantified in each real-time assay together with target gene. Based on gene sequences in GenBank (National Center for Biotechnology Information), the primers for *Nlrp3, Casp1, Il-1β, Il-18, Asc, Il-10, Tnf* , which sequences are presented in **Table 2**, were designed using Primer Express 3.0 software (Applied Biosystems). All reactions were carried out in duplicates in 384-well plate (4309849; Applied Biosystems) in 12 µl of total solution volume (Galvão et al. 2014). The data were analysed using the real-time PCR Miner algorithm (S. Zhao and Fernald 2005).

3.6 ELISA immunoassay

The concentrations of IL-1β in tissue extracts of ovaries and livers were determined using an IL-1 beta Pro-form Mouse Uncoated ELISA kit (88-8014-22; Thermo Fisher Scientific) following

193 manufacturer's instructions. The standard curve concentrations ranged from 25 ng/ml to 3000 ng/m
194 and interassay coefficient variation (CV) was 7.27%.

195 *3.7 Statistical analysis and data presentation*

196 Statistical analyses were performed using the GraphPad Prism Software (Version 7.01, GraphPad
197 Software, Inc.; La Jolla, CA, USA). Paired t test was employed to compare the changes of protein
198 expression in mouse livers and ovaries. Comparisons of gene expression were performed using
199 Wilcoxon matched pairs test. Results are presented as mean with standard deviation. Differences
200 between the means for all tests were considered statistically significant if $p < 0.05$.

201 *2.8 RNA-seq data from CCs*

202 Methods followed the previously described (Wołodko et al. 2020). The GEO accession
203 number for the dataset Sequencing is under submission.

204 **4 Results**

205 *4.1 NLRP3 inflammasome components expression change in the ovary of cyclic mice*

206 We first sought to characterise the expression of NLRP3-induced inflammasome components
207 in the ovaries of mice, throughout the oestrous cycle. Fifteen female 8 wk old C57BL/6 (B6) mice
208 were treated with hormones in order to synchronise oestrous cycle (**Figure 1A**). Mice received either
209 equine chorionic gonadotropin (eCG) or human chorionic gonadotropin (hCG), as previously
210 described (Hasegawa et al. 2016). Ovaries were collected in oestrus (E) and dioestrus (D) stage and
211 further processed for mRNA or protein expression analysis, respectively. Real-time PCR analysis
212 (n=7/group) revealed increased levels of *Casp1*, *Il-1β* and *Il-18* mRNA in D stage (**Figure 1B**,
213 $p<0.05$). Moreover, Western blotting revealed increased NLRP3 protein expression in D (**Figure 1C**,
214 $p<0.05$), as well as the pro-peptide (p24) and mature form (p18) of IL-18 (**Figure 1F, G**; $p<0.01$).

Regarding CASP1, the long form (p45) was decreased in D (**Figure 1D**; $p<0.05$), but no significant changes were observed for the active CASP1 (p20) (**Figure 1E**). These results suggest the activation of NLRP3 inflammasome in D stage, through upregulation of NLRP3 and its downstream mediator IL-18. Next, we characterised the cellular distribution of NLRP3 protein in the ovaries collected from mice in D, using immunohistochemistry (IHC) and immunofluorescence (IF). We confirmed that NLRP3 protein was globally distributed in the ovary (**Figure 1I**). On the other hand, a closer observation with IHC revealed staining in granulosa cells (GC) and theca cells (TC), as well as oocytes, in all developmental stages of follicles in the ovary (**Figure 1K-M**). Negative controls stained with secondary antibodies did not reveal any brown staining (**Figure 1H, J**). The specificity of our IHC staining was corroborated by IF, in which a clear brown staining was observed in GC, TC and oocytes (**Figure 1O-U**). Negative control stained with rabbit immunoglobulin type G (IgG) confirmed no staining (**Figure 1N**). Our results once more corroborate the findings of Zhang and co-workers who not only observed the presence of NLRP3 protein in GC, TC and oocytes by IHC, but also confirmed the upregulation of NLRP3 in the ovaries of eCG treated mice (Z. Zhang, Wang, and Zhang 2019). Therefore, in subsequent experiments, collections were consistently performed in D.

4.2 Time-course activation of NLRP3-induced inflammasome in the ovary of DIO mice

In the following experiment, we tested the effect of short (4 wk) versus long term (16 wk) HFD treatment on NLRP3-induced inflammasome activation in the ovary of mice (**Figure 2A**). We used the DIO protocol previously validated, in which female mice were fed chow diet (CD) or HFD for 4 or 16 wk (n=8/group) (Wołodko et al. 2020). After the DIO protocol, we recorded the average body weight (BW) of 19.7 gram (g) in 4 wk CD group and 24.8 g in 4 wk HFD group, whereas the 16 wk CD presented on average BW of 22.6 g and 16 wk HFD 37.6 g BW (**Table 3**). After collection, ovaries were processed for mRNA and protein expression analysis. Real-time PCR analysis (n=6-8) revealed increased mRNA of *Nlrp3* after 4 wk HFD (**Figure 2B**, $p=0.06$), whereas

Il-1β levels were increased after both 4 wk and 16 wk of HFD (**Figure 2B**, $p<0.05$). Regarding Western blotting analysis (n=8), we found the expression of NLRP3, CASP1 p45 and pro-IL-18 p24 were increased in 4 wk HFD group, compared to control group (**Figure 2C, D**, and **F**, $p<0.05$, respectively). However, opposite pattern was observed in 16 wk HFD, with downregulation of NLRP3 expression, the mature form of CASP1 p20 and both forms of IL-18 (p24 and p18) (**Figure 2 C, E, F** and **G**, $p<0.05$). Finally, we also confirmed IL-1β protein level was upregulated in 16 wk HFD after measurement by enzyme linked immunosorbent assay (ELISA) (n=6) (**Figure 2H**, $p=0.082$). Therefore, we presently confirmed that NLRP3, the pro-proteins IL-18 (p18, p24) and CASP1 (p45) despite being upregulated after 4 wk HFD treatment, after 16 wk HFD treatment a consistent downregulation of NLRP3 inflammasome, particularly NLRP3, CASP1 (p20) and both forms of IL-18, was seen. As a result, increased IL-1β protein after 16 wk HFD should be promoted independently from the NLRP3 inflammasome pathway (Lukens et al. 2014; Ranson et al. 2018).

4.3 Leptin signalling in the ovary drives activation of NLRP3 inflammasome during obesity progression

After temporally characterising the expression profile of NLRP3-induced inflammasome components in the ovary of DIO mice, we further interrogated whether activation of the NLRP3 inflammasome was regulated by leptin signalling. Indeed, leptin was previously shown to modulate NLRP3 expression *in vitro* (Fu et al. 2017). Furthermore, the expression signature of NLRP3 inflammasome components in the ovaries of DIO mice overlapped both tyrosine 985 of leptin receptor (Tyr985ObRb) and Janus kinase 2 (JAK2) phosphorylation profile, with the increase at 4 wk HFD treatment being followed by inhibition at 16 wk HFD and concomitant establishment of leptin resistance (Wołodko et al. 2020). Therefore, we analysed the levels of NLRP3 inflammasome components in the ovaries of a previously validated mouse model of pharmacological hyperleptinemia, which presented increased systemic levels of leptin and increased leptin signalling

in the ovary without obesity (Wołodko et al. 2020), and a genetically obese mouse B6.Cg-Lepob/J (*ob/ob*), characterised by extreme obesity without leptin. In the pharmacological hyperleptinemic model, ten female B6 8 wk old mice, were treated with leptin intraperitoneally, twice a day for 16 days (16 L), whereas controls were administered saline (16 C) (Wołodko et al. 2020). Moreover, ten female *ob/ob* control (+/?) and ten females homozygous mutant (-/-), 8 wk old were kept on CD for 4 wk (**Figure 3A**). Ovaries from all groups were collected and processed for mRNA and protein expression analysis. Real-time PCR analysis (n=6-8/group) revealed an increase in *Nlrp3* and *Casp1* in 16 L, but decrease in *ob/ob* -/- mice (**Figure 3B**, $p<0.05$). Furthermore, mRNA of *Il-1β* was upregulated in 16 L (**Figure 3B**, $p<0.05$). Finally, the mRNA of *Il-18* was significantly downregulated in *ob/ob* -/- group (**Figure 3B**, $p<0.05$). With regard to protein expression, we found the 16 L group presented increased levels of NLRP3 (**Figure 3C**, $p<0.05$), whereas the opposite pattern was observed in *ob/ob* -/- mice, comparing to control groups (**Figure 3C**, $p<0.05$). Accordingly, both pro-peptides CASP1 (p45) and CASP1 (p20) showed increased levels in 16 L (**Figure 3D, E**; $p=0.07$ and $p<0.05$, respectively), nonetheless, no significant changes were found in the *ob/ob* model. Importantly, IL-1β protein measured by ELISA was increased in 16 L, but decreased in *ob/ob* -/- (**Figure 3F**, $p<0.05$). In this experiment we revealed the functional link between leptin signalling and NLRP3 inflammasome components regulation in the ovary, with leptin treatment inducing the activation of NLRP3 and CASP1 with subsequent secretion of IL-1β. Furthermore, the absence of NLRP3 inflammasome activation in the ovary of *ob/ob* -/- confirms the preponderant role active leptin signalling exerts on NLRP3 inflammasome activation in the ovary.

4.4 Leptin promotes changes of NLRP3 inflammasome components gene expression in cumulus cells during early onset of obesity

In this experiment we examined whether the association previously observed between leptin signalling and NLRP3 inflammasome activation found in whole ovaries holds true at the cellular

level, particularly for the somatic companions of the female gamete, the CCs. Indeed, the ovary is a very heterogeneous organ, with follicles in different developmental stages, and different somatic cells supporting oocyte development (Chang, Qiao, and Leung 2017). Therefore, we reanalysed our RNA sequencing (RNA-seq) datasets from CCs from the 4 wk HFD, 16 wk HFD and 16 L groups (Wołodko et al. 2020). Briefly, we collected approximately 50 CCs per animal, after superovulation, and RNA-seq libraries were generated using a Smart-seq2 oligo-dT method (**Figure 4A**; Wołodko et al. 2020). We started confirming the expression level of leptin and NLRP3 pathway components for 16 L and 4 wk HFD. Despite no changes in *Nlrp3* in CCs after 4 wk HFD, the gene was upregulated in 16 L (**Figure 4B**). Certainly, the low coverage of the samples (an average of 5.5 million reads) and the weak expression level of *Nlrp3* in CCs may account for the lack of changes in 4 wk HFD. Nonetheless, the consistent upregulation of various components of the NLRP3 inflammasome, like *Nlrp3* itself, or *Il-18*, *Casp1*, *Il-1β* and *Asc* in 16 L, is suggestive of the stimulatory effect of leptin on the expression of NLRP3 inflammasome genes also in CCs (**Figure 4B**). As previously shown, DESeq analysis revealed 997 differentially expressed genes (DEGs) in 4 wk HFD and 2026 DEGs in 16 L (Wołodko et al. 2020), in comparison to their control groups ($p<0.05$; Wołodko et al. 2020). In the present analysis, we overlapped the DEGs from 4 wk HFD and 16 L and identified seven genes either up- or downregulated in both conditions (**Figure 4C**). Subsequently, we integrated these 14 DEGs with the main components of NLRP3 and leptin signalling pathways (Wołodko et al. 2020) based on the correlation between their expression levels ($p>0.90$), obtaining five clusters, with one of them underscoring the gene interaction between *Casp1*, *phosphatase and tensin homolog (Pten)* and *signal transducer and activator of transcription 5a (Stat5a)*, as well as the link between *Socs3* and *Il-1β*, known as an important axis involved in the mediation of immune response (Chaves de Souza et al. 2013). Importantly, other genes were highlighted in the network, as *solute carrier family 22 member 15 (Slc22a15)*, a cell membrane transporter and metabolic gene (Nigam 2018), or *stress associated endoplasmic reticulum protein 1 (Serp1)* involved in protein unfolding and stress response

(Yamaguchi et al. 1999). Indeed, metabolic performance in the preovulatory follicle is tightly regulated and involves the crosstalk between GC and oocyte (Wołodko et al. 2021). Also, the ER stress is a common feature observed in the ovaries of obese mothers (Robker, Wu, and Yang 2011) (**Figure 4D**). Finally, gene ontology analysis for the presented network revealed three main events, as negative regulation of glucose transport, positive regulation of cytokine biosynthesis and response to ATP (**Figure 4E**, $p<0.05$). Those certainly are key processes for oocyte maturation, as glucose metabolism in GC provides energy supplies for oocyte maturation (Wołodko et al. 2021). Furthermore, energy production through lipid oxidation and ATP production, is also fundamental for oocyte maturation (Wołodko et al. 2021). Finally, we plotted a subset of genes known to directly activate the NLRP3 inflammasome signalling pathway (Weber et al. 2020), particularly regarding the regulation of glutathione, major mediator of NLRP3 signalling (Hughes et al. 2019), as well as other genes involved in the pathway regulation (Barlan et al. 2011; Billon et al. 2019; Guglielmo et al. 2017; Y. He et al. 2016; Hughes et al. 2019; Hughes and O'Neill 2018; Iyer et al. 2013; Jo et al. 2016; Kim et al. 2015; Li et al. 2016; Martine et al. 2019; Mitoma et al. 2013; Palazón-Riquelme et al. 2018; Shuvarikov et al. 2018; X. Wang et al. 2014; Wolf et al. 2016; T. Zhang et al. 2021; Zhou et al. 2010), and confirmed the similarities between 16 L and 4 wk HFD for those gene lists, in opposition to 16 wk HFD (**Figure 4F**). Thus, as presently shown, systemic administration of leptin activated genes from the NLRP3 inflammasome pathway in CCs, corroborating once more the functional link between leptin signalling and NLRP3 inflammasome activation in CCs of DIO mice.

4.5 Time-course activation of NLRP3-induced inflammasome in liver of DIO mice

Different organs can uniquely adapt to systemic insults like obesity (Smith et al. 2018). Therefore, in the last experiment was asked to what extent mounting inflammatory response through NLRP3 inflammasome activation in the ovaries of DIO mice precede other metabolic organs like the liver. We analysed the expression profile of NLRP3 inflammasome genes in the liver of DIO mice,

besides testing once more the functional link between leptin signalling and activation of NLRP3 inflammasome at hepatic level, using pharmacological hyperleptinemic and *ob/ob* mouse models. Liver samples were collected from DIO, leptin treated and *ob/ob* female mice, for mRNA transcription and protein expression analysis (**Figure 5A**). Real-time PCR analysis (n=5-7/group) showed no significant changes in expression of all inflammasome components, except for the increase of *Nlrp3* and *Il-1β* mRNA in 16 wk HFD, but downregulation of *Nlrp3* in *ob/ob*-/- (**Figure 5B**, $p<0.05$). Furthermore, protein analysis determined by Western blotting (n=4-8/group) showed an increase in protein levels of NLRP3, CASP1 (p20), and IL-18 (p18) after 16 wk HFD treatment, comparing to control (**Figure 5C, E** and **G**, $p=0.07$, $p<0.05$). Regarding the pro-peptide of CASP1 (p45), its protein was upregulated in 16 L, but downregulated in *ob/ob* -/-, comparing to controls (**Figure 5D**, $p<0.05$ and $p<0.01$, respectively). Finally, CASP1 (p20) and IL-18 (p18) proteins were decreased in *ob/ob*-/- (**Figure 5E, G**, $p<0.05$ and $p=0.08$, respectively). No significant changes were observed for pro-IL-18 (p24). The present results on our analysis in the liver indicate a site dependent NLRP3 inflammasome regulation throughout obesity, since overexpression of NLRP3, CASP1 (p20) and IL-18 (p18) took place only at 16 wk of DIO. Differences in NLRP3 inflammasome profile between liver and ovary certainly relay on the intrinsic immunological complexity the liver presents. The liver, in opposition to the ovary, is constantly exposed to proinflammatory mediators, having developed the ability to tightly control inflammation (Robinson, Harmon, and O'Farrelly 2016). Another important observation was the downregulation of NLRP3 and CASP1 (p20) in livers from *ob/ob* -/- mice. Other studies corroborated these observations (Negrin et al. 2014), and despite all intricacies of NLRP3 inflammasome regulation, leptin seems to directly modulate NLRP3 inflammasome activation at hepatic level. Hence, we confirmed the latency of NLRP3 inflammasome activation in the liver of DIO female mice, which showed signs of upregulation only after 16 wk HFD treatment. Furthermore, we have confirmed the functional link between leptin and NLRP3 inflammasome activation in the liver.

5 Discussion

The present study gives the first characterisation of NLRP3 induced inflammasome activation in the ovaries of DIO mice. Maternal obesity has been largely associated with increased ovarian inflammation (J. Nteeba et al. 2013; Jackson Nteeba, Ganesan, and Keating 2014; Robker, Wu, and Yang 2011; Ruebel et al. 2017; Snider and Wood 2019), being a better knowledge of its pathogenesis of undeniable value for our understanding of ovarian failure and infertility during obesity. We firstly confirmed the effects of cyclicity on NLRP3 inflammasome activation in the ovaries of lean mice, observing the upregulation of NLRP3 inflammasome components in D. Subsequently, we temporally characterised the expression profile of NLRP3 inflammasome components in the ovary, throughout obesity progression. Indeed, the rapid upregulation of NLRP3 protein in early obesity (after 4 wk HFD treatment), was followed by a consistent downregulation of NLRP3 inflammasome components, as NLRP3 and CASP1, in late obesity (after 16 wk HFD). Importantly, using either a pharmacological hyperleptinemic and a genetic obese *ob/ob* mouse, we not only evidenced the functional link between levels of leptin signalling and NLRP3 activation in whole ovaries, but also the role of leptin on *Nlrp3*, *Il-18 and Il-1β* gene expression upregulation in CCs from ovulated follicles. Finally, after analysing the NLRP3 inflammasome expression pattern in the liver, we confirmed NLRP3 and CASP1 overexpression took place exclusively after 16 wk HFD treatment, suggesting a delayed activation of NLRP3 inflammasome activation in comparison with the ovary. Hence, these results suggest a greater vulnerability of the ovaries in general, and the gamete in particular, to the energetic surplus females face under obesogenic conditions.

A recent study by Zhang and colleagues evidenced for the first time NLRP3 expression in various cellular components like GC, TC and oocytes of mouse ovaries (Z. Zhang, Wang, and Zhang 2019). We presently confirmed not only the similar pattern of cellular expression for NLRP3, but also the upregulation of NLRP3 inflammasome components during D. These findings corroborate

385 previous results suggesting the involvement of NLRP3 in inflammation during ovulation in mice (Z.
386 Zhang, Wang, and Zhang 2019). Furthermore, NLRP3 proinflammatory role in ovarian function
387 starts getting noticed not only under physiological context (Z. Zhang, Wang, and Zhang 2019), but
388 also as an important mediator of ovarian pathology during ageing (Navarro-Pando et al. 2021).
389 Certainly, our hypothesis of NLRP3 inflammasome involvement in inflammatory response in the
390 ovary of obese mothers seems to be supported also by earlier reports showing NLRP3 inflammasome
391 activation during development and treatment of PCOS (Guo et al. 2020; F. Wang et al. 2017).

392 The NLRP3 inflammasome is a critical component of innate immunity, frequently associated
393 with human disease (Y. He, Hara, and Núñez 2016). Our results evidencing NLRP3 inflammasome
394 activation in the ovaries of 4 wk HFD treatment are in line with previous reports showing the
395 accumulation of proinflammatory mediators in the ovary after short term (6 wk HFD) dietary
396 protocols (Shen, Xu, and Li 2021). Indeed, we presently observed the upregulation of IL-18 protein,
397 as well as increased mRNA of *Tnf* (data not shown), after 4 wk HFD underscoring the mounting
398 inflammatory response. Nonetheless, maintenance of inflammation in the ovaries in long term DIO
399 mice (after 16 wk HFD) seems to be mediated independently from NLRP3 inflammasome pathway,
400 as IL-18 and CASP1 mature proteins were significantly downregulated at this time point.
401 Undeniably, increased levels of IL-1β in the ovaries of 16 wk HFD mice confirm the
402 proinflammatory state in the ovaries of DIO mice after 16 wk HFD, supported by several studies in
403 mice showing the abundancy of inflammatory markers like *Il-1β*, *Il-6* and *Tnfα* and in the ovary of
404 long term DIO mice fed for 24 wk HFD (J. Nteeba et al. 2013). As a result, the increased levels of
405 IL-1β at 16 wk HFD confirm the existence of alternative pathways to NLRP3 inflammasome,
406 mediating IL-1β upregulation (Donado et al. 2020; Jain et al. 2020; Pyrillou, Burzynski, and Clarke
407 2020; Schmidt and Lenz 2012; Zhu and Kanneganti 2017). To this extent, we have recently shown
408 the temporal pattern of expression of proinflammatory genes in CCs from DIO mice (Wołodko et al.

2020). In early obesity, inflammatory cues in CCs were mediated by cellular response to stress through upregulation of genes like *DEAD-box helicase 5 (Ddx5), hypoxia inducible factor 1 subunit alpha (Hif1a), ADAM metallopeptidase domain 9 (Adam9*). Indeed, mediators of stress response as ROS are known to prime the NLRP3 inflammasome (Gurung et al. 2014). Subsequently, in late obesity, we saw the overexpression of genes involved in anatomical structural morphogenesis, as *C-C motif chemokine ligand 7* (*Ccl7*), an important chemoattractant of leukocytes (Menten et al. 1999), and also known to interact with matrix metalloproteinases (MMPs) (Liu et al. 2018), or complement C3a receptor 1 (*C3ar1*), a complement component known to mediate neutrophil mobilisation (Brennan et al. 2019) and lately described as a marker of PCOS progression (D. He et al. 2020). Therefore, these data suggest important temporal dynamics on the regulation of the inflammatory response in the ovary throughout obesity progression, with NLRP3 inflammasome playing a critical role mostly in the initiation of inflammation in the ovaries in early obesity. Conversely, in late obesity, immune mediated response in the ovary progresses to infiltration of immune cells and structural reorganisation, independently from the activation of NLRP3 inflammasome.

Our study also sheds light on the important crosstalk between leptin signalling and inflammasome NLRP3 activation in the ovary of DIO mice. As reviewed by Wani and co-workers, numerous factors were shown to activate NLRP3 inflammasome during obesity, such as cellular metabolites, carbohydrates or lipids (Wani et al. 2021). Nonetheless, leptin, a conserved proinflammatory cytokine (Iikuni et al. 2008; La Cava 2017), was recently shown to upregulated NLRP3 components *in vitro* (Fu et al. 2017). Thus, in order to test the hypothesis whether repression of NLRP3 inflammasome activation in ovaries of 16 wk HFD mice was due to the establishment of leptin resistance (Wołodko et al. 2020), we studied NLRP3 inflammasome activation in the ovaries of pharmacological hyperleptinemic and *ob/ob* mice. Strikingly, we observed a consistent upregulation of NLRP3 inflammasome genes and accumulation of IL-1β protein in ovaries of leptin

433 treated mice, in opposition to *ob/ob* -/- mice which evidenced consistent downregulation of NLRP3
434 and IL-1β proteins. Furthermore, reduced levels of NLRP3 were also observed in *ob/ob* -/- mouse
435 peritoneal macrophages treated with LPS and nigericin in comparison to wild type mice (Yang et al.
436 2021), what certainly underlines the preponderant role of leptin on NLRP3 inflammasome regulation.
437 Therefore, our results invite us to suggest the activation of NLRP3 inflammasome in the ovary of
438 DIO mice is mediated by leptin signalling. In early obesity (4 wk HFD treatment) leptin actively
439 signals through receptor b (ObRb) in the ovary (Wołodko et al. 2020), with the overexpression of
440 NLRP3 inflammasome components; nonetheless, in late obesity (16 wk HFD treatment) after the
441 establishment of leptin resistance in the organ (Wołodko et al. 2020), expression of NLRP3
442 inflammasome is drastically repressed.

443 Next, we reanalysed our datasets on global gene expression in CCs collected from
444 pharmacological hyperleptinemic and DIO mice, in order to test the association between leptin
445 signalling and activation of NLRP3 inflammasome in the somatic companions of the oocyte.
446 Importantly, CCs are known as faithful indicators of intrafollicular environment (Wołodko et al.
447 2021) and their transcriptome has been used to predict oocyte and embryo quality (Uyar, Torrealday,
448 and Seli 2013). Despite no changes in 4 wk HFD, we confirmed the overexpression of NLRP3
449 inflammasome genes in CCs from 16 L. Consequently, we interrogated whether DEGs overlapping
450 both 16 L and 4 wk HFD treatment could interacted with NLRP3 inflammasome genes. Indeed gene
451 ontology for associated genes revealed key terms for oocyte maturation, as regulation of glucose
452 transport, response to ATP and regulation of cytokine biosynthesis. Metabolic regulation in
453 preovulatory follicles appears to control major steps for maturation of female gamete, as meiosis
454 resumption, chromatin condensation and cytoplasm maturation (Wołodko et al. 2021). For instance,
455 glucose, which is mostly metabolised in CCs (Sanfins, Rodrigues, and Albertini 2018) was shown to
456 be key for oocyte competence (Wilding et al. 2009), as well as reduced ATP content in oocytes was

457 linked to failure in fertilisation, arrested division and abnormal embryonic development (J. Zhao and
458 Li 2012). Furthermore, the aforementioned involvement of NLRP3 inflammasome in ovulation (Z.
459 Zhang, Wang, and Zhang 2019) can be considered amongst the regulation of the cytokine milieu
460 locally produced in CCs. Given leptin direct and indirect role in ovulation (Wołodko et al. 2021),
461 failure in leptin signalling and NLRP3 inflammasome activation in late obesity can account for
462 increased anovulatory rates in obese mothers (Hou et al. 2016; Wu et al. 2010). Finally, absence of
463 changes in 4 wk HFD in NLRP3 inflammasome genes can be ascribed to low coverage of our
464 reduced-cell libraries and also low levels of gene expression. Indeed, the present RNA-seq protocol
465 used as little as 50 cells per mouse, which has limitations while analysing weakly expressed genes.
466 Collectively, our results indicate leptin and NLRP3 inflammasome crosstalk in CCs can interfere
467 with major steps regulating oocyte maturation and early embryo development.

468 In the last experiment we confirmed the liver, in sharp contrast to the ovary, activated NLRP3
469 inflammasome later in time during DIO protocol (after 16 wk HFD treatment) in mice. Temporal
470 differences in inflammatory response regulation between both organs certainly rely on contrasting
471 exposition to exogenous pathogens. The liver is an organ constantly exposed to proinflammatory
472 mediators from dietary and commensal bacterial products (Robinson, Harmon, and O'Farrelly 2016).
473 Thus, the hepatic immune system is constantly in contact with altered metabolic activity and regular
474 exposition to microbial products, which results in persistent and tightly regulated inflammatory
475 response (Robinson, Harmon, and O'Farrelly 2016). On the contrary, the ovary is not only a highly
476 immunogenic organ constantly secreting large amounts of cytokines and immune mediators (Piccinni
477 et al. 2021), but also more prone to rapidly mounting proinflammatory response during obesity.
478 Indeed, the inability of the ovary to control inflammation and exacerbated cytokine production
479 certainly ascribes for the great vulnerability the female gamete presents to maternal obesity even at

earlier stages. Thus, our results expose the increased ovarian vulnerability to maternal obesity, with a rapid mounting inflammation which affects the gamete and impairs fertilisation.

In summary, our work evidences the major role leptin signalling exerts on NLRP3 inflammasome activity in the ovary of obese mice. Noteworthy, failure in ovarian leptin signalling was associated with repression in NLRP3 activity, but not decreased inflammation and levels of IL-1β. Moreover, NLRP3 inflammasome activation in the ovary precedes liver response during obesity progression suggesting the greater vulnerability the ovary in general, and gamete in particular, to the energetic surplus during maternal obesity.

Conflict of Interest

The authors have no conflict of interest to declare.

Author Contributions

MA did data acquisition, analysis and interpretation of the data, writing the manuscript; KW did data acquisition and analysis and revised and edited the manuscript; JO did immunohistochemistry staining; JCF conducted data analysis and interpretation of data, revising the manuscript; DM did immunohistochemistry staining; GK revised and edited the manuscript; AG conceptualised and designed the study, acquired the funding, participated in data acquisition, analysis and interpretation, and wrote and edited the manuscript.

Funding

Work supported by grants from the Polish National Science Centre (No. 2016/23/B/NZ4/03737 and 2019/34/E/NZ4/00349) awarded to A. G.; A. G. was supported by Horizon 2020 Marie Curie Individual Fellowship (MOBER, 2017-2019) and by the KNOW Consortium: “Healthy Animal - Safe Food” (Ministry of Sciences and Higher Education; Dec: 05-1/KNOW2/2015).

Acknowledgments

We would like to thank Dr Leslie Paul Kozak and Dr Magdalena Jura for their support with the validation and characterisation of the mouse obese phenotype; and Dr Krzysztof Witek for his support with the imaging and confocal microscopy.

Data Availability Statement

The raw data supporting the conclusions of this article were made available within the publication Wołodko et al 2020.

References

Barlan, A. U., T. M. Griffin, K. A. McGuire, and C. M. Wiethoff. 2011. 'Adenovirus Membrane Penetration Activates the NLRP3 Inflammasome'. *Journal of Virology* 85 (1): 146–55. https://doi.org/10.1128/JVI.01265-10.

Billon, Cyrielle, Meghan H. Murray, Amer Avdagic, and Thomas P. Burris. 2019. 'RORγ Regulates the NLRP3 Inflammasome'. *The Journal of Biological Chemistry* 294 (1): 10–19. https://doi.org/10.1074/jbc.AC118.002127.

Boden, Guenther. 2002. 'Interaction between Free Fatty Acids and Glucose Metabolism'. *Current Opinion in Clinical Nutrition and Metabolic Care* 5 (5): 545–49. https://doi.org/10.1097/00075197-200209000-00014.

Brennan, Faith H., Trisha Jogia, Ellen R. Gillespie, Linda V. Blomster, Xaria X. Li, Bianca Nowlan, Gail M. Williams, et al. 2019. 'Complement Receptor C3aR1 Controls Neutrophil Mobilization Following Spinal Cord Injury through Physiological Antagonism of CXCR2'. *JCI Insight* 4 (9). https://doi.org/10.1172/jci.insight.98254.

Cauble, Reagan, S. Hamad, Ellen Herring, Callan Lichtenwalter, C. McGuire, and Sami Dridi. 2018. 'Leptin Activates NLRP3 Inflammasome-Associated with Type II Diabetes and Obesity'. *Advances in Food Technology and Nutritional Sciences - Open Journal* 4 (November): e13–16. https://doi.org/10.17140/AFTNSOJ-4-e016.

Chang, Hsun-Ming, Jie Qiao, and Peter C.K. Leung. 2017. 'Oocyte–Somatic Cell Interactions in the Human Ovary—Novel Role of Bone Morphogenetic Proteins and Growth Differentiation Factors'. *Human Reproduction Update* 23 (1): 1–18. https://doi.org/10.1093/humupd/dmw039.

Chaves de Souza, João Antônio, Andressa Vilas Boas Nogueira, Pedro Paulo Chaves de Souza, Yeon Jung Kim, Caroline Silva Lobo, Guilherme José Pimentel Lopes de Oliveira, Joni Augusto Cirelli, Gustavo Pompermaier Garlet, and Carlos Rossa. 2013. 'SOCS3 Expression Correlates with Severity of Inflammation, Expression of Proinflammatory Cytokines, and Activation of STAT3 and P38 MAPK in LPS-Induced Inflammation In Vivo'. *Mediators of Inflammation* 2013. https://doi.org/10.1155/2013/650812.

Chu, Susan Y., Shin Y. Kim, Joseph Lau, Christopher H. Schmid, Patricia M. Dietz, William M. Callaghan, and Kathryn M. Curtis. 2007. 'Maternal Obesity and Risk of Stillbirth: A Metaanalysis'. *American Journal of Obstetrics and Gynecology* 197 (3): 223–28. https://doi.org/10.1016/j.ajog.2007.03.027.

Davis, Beckley K., Haitao Wen, and Jenny P.-Y. Ting. 2011. 'The Inflammasome NLRs in Immunity, Inflammation, and Associated Diseases'. *Annual Review of Immunology* 29: 707–35. https://doi.org/10.1146/annurev-immunol-031210-101405.

De Nardo, Dominic, and Eicke Latz. 2011. 'NLRP3 Inflammasomes Link Inflammation and Metabolic Disease'. *Trends in Immunology* 32 (8): 373–79. https://doi.org/10.1016/j.it.2011.05.004.

Donado, Carlos A., Anh B. Cao, Daimon P. Simmons, Ben A. Croker, Patrick J. Brennan, and Michael B. Brenner. 2020. 'A Two-Cell Model for IL-1β Release Mediated by Death-Receptor Signaling'. *Cell Reports* 31 (1): 107466. https://doi.org/10.1016/j.celrep.2020.03.030.

564 Fu, Sisi, Lei Liu, Lei Han, and Yiyun Yu. 2017. 'Leptin Promotes IL‐18 Secretion by Activating the
565 NLRP3 Inflammasome in RAW 264.7 Cells'. *Molecular Medicine Reports* 16 (6): 9770–76.
566 https://doi.org/10.3892/mmr.2017.7797.
567 Galvão, António, Sofia Henriques, Daria Pestka, Karolina Lukasik, Dariusz Skarzynski, Luisa Maria
568 Mateus, and Graça Maria Leitao Ferreira-Dias. 2012. 'Equine Luteal Function Regulation
569 May Depend on the Interaction between Cytokines and Vascular Endothelial Growth Factor:
570 An in Vitro Study'. *Biology of Reproduction* 86 (6): 187.
571 https://doi.org/10.1095/biolreprod.111.097147.
572 Galvão, António, Angela Tramontano, Maria Rosa Rebordão, Ana Amaral, Pedro Pinto Bravo, Anna
573 Szóstek, Dariusz Skarzynski, Antonio Mollo, and Graça Ferreira-Dias. 2014. 'Opposing
574 Roles of Leptin and Ghrelin in the Equine Corpus Luteum Regulation: An In Vitro Study'.
575 *Mediators of Inflammation* 2014 (July): e682193. https://doi.org/10.1155/2014/682193.
576 Guglielmo, Andrew, Adham Sabra, Mostafa Elbery, Milena M. Cerveira, Fernanda Ghenov, Rajesh
577 Sunasee, and Karina Ckless. 2017. 'A Mechanistic Insight into Curcumin Modulation of the
578 IL-1β Secretion and NLRP3 S-Glutathionylation Induced by Needle-like Cationic Cellulose
579 Nanocrystals in Myeloid Cells'. *Chemico-Biological Interactions* 274 (August): 1–12.
580 https://doi.org/10.1016/j.cbi.2017.06.028.
581 Guo, Qing-Jun, Jing Shan, Yi-Feng Xu, Yan-Yan Hu, Cui-Lan Huo, Jing-Yun Song, Chao-Qun
582 Wang, Hui Zhou, Chao-Qin Yu, and Qin Huang. 2020. 'Pioglitazone Metformin Complex
583 Improves Polycystic Ovary Syndrome Comorbid Psychological Distress via Inhibiting
584 NLRP3 Inflammasome Activation: A Prospective Clinical Study'. *Mediators of Inflammation*
585 2020: 3050487. https://doi.org/10.1155/2020/3050487.
586 Gurung, Prajwal, Paras K. Anand, R. K. Subbarao Malireddi, Lieselotte Vande Walle, Nina Van
587 Opdenbosch, Christopher P. Dillon, Ricardo Weinlich, Douglas R. Green, Mohamed
588 Lamkanfi, and Thirumala-Devi Kanneganti. 2014. 'FADD and Caspase-8 Mediate Priming
589 and Activation of the Canonical and Noncanonical Nlrp3 Inflammasomes'. *Journal of*
590 *Immunology (Baltimore, Md.: 1950)* 192 (4): 1835–46.
591 https://doi.org/10.4049/jimmunol.1302839.
592 Hasegawa, Ayumi, Keiji Mochida, Hiroki Inoue, Yoshihiro Noda, Tamao Endo, Gen Watanabe, and
593 Atsuo Ogura. 2016. 'High-Yield Superovulation in Adult Mice by Anti-Inhibin Serum
594 Treatment Combined with Estrous Cycle Synchronization1'. *Biology of Reproduction* 94 (21,
595 1–8). https://doi.org/10.1095/biolreprod.115.134023.
596 He, Dongyun, Li Liu, Yang Wang, and Minjia Sheng. 2020. 'A Novel Genes Signature Associated
597 with the Progression of Polycystic Ovary Syndrome'. *Pathology Oncology Research: POR* 26
598 (1): 575–82. https://doi.org/10.1007/s12253-019-00676-3.
599 He, Yuan, Hideki Hara, and Gabriel Núñez. 2016. 'Mechanism and Regulation of NLRP3
600 Inflammasome Activation'. *Trends in Biochemical Sciences* 41 (12): 1012–21.
601 https://doi.org/10.1016/j.tibs.2016.09.002.
602 He, Yuan, Melody Y. Zeng, Dahai Yang, Benny Motro, and Gabriel Núñez. 2016. 'NEK7 Is an
603 Essential Mediator of NLRP3 Activation Downstream of Potassium Efflux'. *Nature* 530
604 (7590): 354–57. https://doi.org/10.1038/nature16959.
605 Hotamisligil, Gökhan S., and Ebru Erbay. 2008. 'Nutrient Sensing and Inflammation in Metabolic
606 Diseases'. *Nature Reviews Immunology* 8 (12): 923–34. https://doi.org/10.1038/nri2449.
607 Hou, Yan-Jun, Cheng-Cheng Zhu, Xing Duan, Hong-Lin Liu, Qiang Wang, and Shao-Chen Sun.
608 2016. 'Both Diet and Gene Mutation Induced Obesity Affect Oocyte Quality in Mice'.
609 *Scientific Reports* 6 (1): 18858. https://doi.org/10.1038/srep18858.
610 Hughes, Mark M., Alexander Hooftman, Stefano Angiari, Padmaja Tummala, Zbigniew Zaslona,
611 Marah C. Runtsch, Anne F. McGettrick, et al. 2019. 'Glutathione Transferase Omega-1

Regulates NLRP3 Inflammasome Activation through NEK7 Deglutathionylation'. *Cell Reports* 29 (1): 151-161.e5. https://doi.org/10.1016/j.celrep.2019.08.072.

Hughes, Mark M., and Luke A. J. O'Neill. 2018. 'Metabolic Regulation of NLRP3'. *Immunological Reviews* 281 (1): 88–98. https://doi.org/10.1111/imr.12608.

Iikuni, Noriko, Queenie Lai Kwan Lam, Liwei Lu, Giuseppe Matarese, and Antonio La Cava. 2008. 'Leptin and Inflammation'. *Current Immunology Reviews* 4 (2): 70–79. https://doi.org/10.2174/157339508784325046.

Iyer, Shankar S., Qiong He, John R. Janczy, Eric I. Elliott, Zhenyu Zhong, Alicia K. Olivier, Jeffrey J. Sadler, et al. 2013. 'Mitochondrial Cardiolipin Is Required for Nlrp3 Inflammasome Activation'. *Immunity* 39 (2): 311–23. https://doi.org/10.1016/j.immuni.2013.08.001.

Jain, Aakanksha, Ricardo A. Irizarry-Caro, Margaret M. McDaniel, Amanpreet Singh Chawla, Kaitlin R. Carroll, Garrett R. Overcast, Naomi H. Philip, et al. 2020. 'T Cells Instruct Myeloid Cells to Produce Inflammasome-Independent IL-1β and Cause Autoimmunity'. *Nature Immunology* 21 (1): 65–74. https://doi.org/10.1038/s41590-019-0559-y.

Jo, Eun-Kyeong, Jin Kyung Kim, Dong-Min Shin, and Chihiro Sasakawa. 2016. 'Molecular Mechanisms Regulating NLRP3 Inflammasome Activation'. *Cellular and Molecular Immunology* 13 (2): 148–59. https://doi.org/10.1038/cmi.2015.95.

Jungheim, Emily S., Erica L. Schoeller, Kerri L. Marquard, Erica D. Louden, Jean E. Schaffer, and Kelle H. Moley. 2010. 'Diet-Induced Obesity Model: Abnormal Oocytes and Persistent Growth Abnormalities in the Offspring'. *Endocrinology* 151 (8): 4039–46. https://doi.org/10.1210/en.2010-0098.

Kim, So Ri, Yong Chul Lee, Hee Jung Kim, and Soon Ha Kim. 2015. 'Activation of NLRP3 Inflammasome Is Regulated by Mitochondrial ROS via PI3K-HIF-VEGF Pathway in Acute Lung Injury'. *European Respiratory Journal* 46 (suppl 59). https://doi.org/10.1183/13993003.congress-2015.PA3026.

Krebs, M., and M. Roden. 2005. 'Molecular Mechanisms of Lipid-Induced Insulin Resistance in Muscle, Liver and Vasculature'. *Diabetes, Obesity & Metabolism* 7 (6): 621–32. https://doi.org/10.1111/j.1463-1326.2004.00439.x.

Kyrönlahti, Antti, Melanie Vetter, Rosemarie Euler, Malgorzata Bielinska, Patrick Y. Jay, Mikko Anttonen, Markku Heikinheimo, and David B. Wilson. 2011. 'GATA4 Deficiency Impairs Ovarian Function in Adult Mice'. *Biology of Reproduction* 84 (5): 1033–44. https://doi.org/10.1095/biolreprod.110.086850.

La Cava, Antonio. 2017. 'Leptin in Inflammation and Autoimmunity'. *Cytokine* 98 (October): 51–58. https://doi.org/10.1016/j.cyto.2016.10.011.

Lamkanfi, Mohamed. 2011. 'Emerging Inflammasome Effector Mechanisms'. *Nature Reviews Immunology* 11 (3): 213–20. https://doi.org/10.1038/nri2936.

Lamkanfi, Mohamed, and Vishva M. Dixit. 2014. 'Mechanisms and Functions of Inflammasomes'. *Cell* 157 (5): 1013–22. https://doi.org/10.1016/j.cell.2014.04.007.

Li, Yi, Jia-Yi Zheng, Jian-Qun Liu, Jie Yang, Yang Liu, Chen Wang, Xiao-Nan Ma, Bao-Lin Liu, Gui-Zhong Xin, and Li-Fang Liu. 2016. 'Succinate/NLRP3 Inflammasome Induces Synovial Fibroblast Activation: Therapeutical Effects of Clematichinenoside AR on Arthritis'. *Frontiers in Immunology* 7 (December). https://doi.org/10.3389/fimmu.2016.00532.

Liu, Yangyang, Yadi Cai, Li Liu, Yudong Wu, and Xiangyang Xiong. 2018. 'Crucial Biological Functions of CCL7 in Cancer'. *PeerJ* 6: e4928. https://doi.org/10.7717/peerj.4928.

Lukens, John R., Jordan M. Gross, Christopher Calabrese, Yoichiro Iwakura, Mohamed Lamkanfi, Peter Vogel, and Thirumala-Devi Kanneganti. 2014. 'Critical Role for Inflammasome-Independent IL-1β Production in Osteomyelitis'. *Proceedings of the National Academy of Sciences* 111 (3): 1066–71. https://doi.org/10.1073/pnas.1318688111.

Martine, Pierre, Angélique Chevriaux, Valentin Derangère, Lionel Apetoh, Carmen Garrido, François Ghiringhelli, and Cédric Rébé. 2019. 'HSP70 Is a Negative Regulator of NLRP3 Inflammasome Activation'. *Cell Death & Disease* 10 (4): 1–11. https://doi.org/10.1038/s41419-019-1491-7.

Martinon, Fabio, Kimberly Burns, and Jürg Tschopp. 2002. 'The Inflammasome: A Molecular Platform Triggering Activation of Inflammatory Caspases and Processing of ProIL-Beta'. *Molecular Cell* 10 (2): 417–26. https://doi.org/10.1016/s1097-2765(02)00599-3.

Martinon, Fabio, Virginie Pétrilli, Annick Mayor, Aubry Tardivel, and Jürg Tschopp. 2006. 'Gout-Associated Uric Acid Crystals Activate the NALP3 Inflammasome'. *Nature* 440 (7081): 237–41. https://doi.org/10.1038/nature04516.

Menten, P., P. Proost, S. Struyf, E. Van Coillie, W. Put, J. P. Lenaerts, R. Conings, et al. 1999. 'Differential Induction of Monocyte Chemotactic Protein-3 in Mononuclear Leukocytes and Fibroblasts by Interferon-Alpha/Beta and Interferon-Gamma Reveals MCP-3 Heterogeneity'. *European Journal of Immunology* 29 (2): 678–85. https://doi.org/10.1002/(SICI)1521-4141(199902)29:02<678::AID-IMMU678>3.0.CO;2-J.

Minge, Cadence E., Brenton D. Bennett, Robert J. Norman, and Rebecca L. Robker. 2008. 'Peroxisome Proliferator-Activated Receptor-Gamma Agonist Rosiglitazone Reverses the Adverse Effects of Diet-Induced Obesity on Oocyte Quality'. *Endocrinology* 149 (5): 2646–56. https://doi.org/10.1210/en.2007-1570.

Mitoma, Hiroki, Shino Hanabuchi, Taeil Kim, Musheng Bao, Zhiqiang Zhang, Naoshi Sugimoto, and Yong-Jun Liu. 2013. 'The DEAH Box RNA Helicase DHX33 Senses Cytosolic RNA and Activates the NLRP3 Inflammasome'. *Immunity* 39 (1): 123–35. https://doi.org/10.1016/j.immuni.2013.07.001.

Navarro-Pando, José M., Elísabet Alcocer-Gómez, Beatriz Castejón-Vega, Elena Navarro-Villarán, Mónica Condés-Hervás, María Mundi-Roldan, Jordi Muntané, et al. 2021. 'Inhibition of the NLRP3 Inflammasome Prevents Ovarian Aging'. *Science Advances* 7 (1): eabc7409. https://doi.org/10.1126/sciadv.abc7409.

Negrin, Kimberly A., Rachel J. Roth Flach, Marina T. DiStefano, Anouch Matevossian, Randall H. Friedline, DaeYoung Jung, Jason K. Kim, and Michael P. Czech. 2014. 'IL-1 Signaling in Obesity-Induced Hepatic Lipogenesis and Steatosis'. *PLOS ONE* 9 (9): e107265. https://doi.org/10.1371/journal.pone.0107265.

Nigam, Sanjay K. 2018. 'The SLC22 Transporter Family: A Paradigm for the Impact of Drug Transporters on Metabolic Pathways, Signaling, and Disease'. *Annual Review of Pharmacology and Toxicology* 58 (January): 663–87. https://doi.org/10.1146/annurev-pharmtox-010617-052713.

Nteeba, J., L. C. Ortinau, J. W. Perfield, and A. F. Keating. 2013. 'Diet-Induced Obesity Alters Immune Cell Infiltration and Expression of Inflammatory Cytokine Genes in Mouse Ovarian and Peri-Ovarian Adipose Depot Tissues'. *Molecular Reproduction and Development* 80 (11): 948–58. https://doi.org/10.1002/mrd.22231.

Nteeba, Jackson, Shanthi Ganesan, and Aileen F. Keating. 2014. 'Progressive Obesity Alters Ovarian Folliculogenesis with Impacts on Pro-Inflammatory and Steroidogenic Signaling in Female Mice1'. *Biology of Reproduction* 91 (86, 1–11). https://doi.org/10.1095/biolreprod.114.121343.

Odegaard, Justin I., and Ajay Chawla. 2008. 'Mechanisms of Macrophage Activation in Obesity-Induced Insulin Resistance'. *Nature Clinical Practice. Endocrinology & Metabolism* 4 (11): 619–26. https://doi.org/10.1038/ncpendmet0976.

Palazón-Riquelme, Pablo, Jonathan D Worboys, Jack Green, Ana Valera, Fatima Martín-Sánchez, Carolina Pellegrini, David Brough, and Gloria López-Castejón. 2018. 'USP7 and USP47

Deubiquitinases Regulate NLRP3 Inflammasome Activation'. *EMBO Reports* 19 (10): e44766. https://doi.org/10.15252/embr.201744766.

Penzias, Alan S. 2012. 'Recurrent IVF Failure: Other Factors'. *Fertility and Sterility* 97 (5): 1033–38. https://doi.org/10.1016/j.fertnstert.2012.03.017.

Piccinni, Marie-Pierre, Rossella Vicenti, Federica Logiodice, Raffaella Fabbri, Ornela Kullolli, Marco Pallecchi, Roberto Paradisi, et al. 2021. 'Description of the Follicular Fluid Cytokine and Hormone Profiles in Human Physiological Natural Cycles'. *The Journal of Clinical Endocrinology & Metabolism* 106 (2): e721–38. https://doi.org/10.1210/clinem/dgaa880.

Pyrillou, Katerina, Laura C. Burzynski, and Murray C. H. Clarke. 2020. 'Alternative Pathways of IL-1 Activation, and Its Role in Health and Disease'. *Frontiers in Immunology* 11. https://doi.org/10.3389/fimmu.2020.613170.

Ranson, Nicole, Mark Veldhuis, Brent Mitchell, Scott Fanning, Anthony L. Cook, Dale Kunde, and Rajaraman Eri. 2018. 'NLRP3-Dependent and -Independent Processing of Interleukin (IL)-1β in Active Ulcerative Colitis'. *International Journal of Molecular Sciences* 20 (1). https://doi.org/10.3390/ijms20010057.

Robinson, Mark W., Cathal Harmon, and Cliona O'Farrelly. 2016. 'Liver Immunology and Its Role in Inflammation and Homeostasis'. *Cellular & Molecular Immunology* 13 (3): 267–76. https://doi.org/10.1038/cmi.2016.3.

Robker, Rebecca L. 2008. 'Evidence That Obesity Alters the Quality of Oocytes and Embryos'. *Pathophysiology: The Official Journal of the International Society for Pathophysiology* 15 (2): 115–21. https://doi.org/10.1016/j.pathophys.2008.04.004.

Robker, Rebecca L., Linda L. -Y. Wu, and Xing Yang. 2011. 'Inflammatory Pathways Linking Obesity and Ovarian Dysfunction'. *Journal of Reproductive Immunology*, XI International Congress of Reproductive Immunology, 88 (2): 142–48. https://doi.org/10.1016/j.jri.2011.01.008.

Rostamtabar, Maryam, Sedighe Esmaeilzadeh, Ahmad Karkhah, Mania Amiri, Abolfazl Rahmani, Fatemeh Bakouei, and Hamid Reza Nouri. 2020. 'Elevated Expression of IL-18 but Not IL-1β Gene Is Associated with NALP3 and AIM2 Inflammasome in Polycystic Ovary Syndrome'. *Gene* 731 (March): 144352. https://doi.org/10.1016/j.gene.2020.144352.

Ruebel, Meghan L., Matthew Cotter, Clark R. Sims, Dean M. Moutos, Thomas M. Badger, Mario A. Cleves, Kartik Shankar, and Aline Andres. 2017. 'Obesity Modulates Inflammation and Lipid Metabolism Oocyte Gene Expression: A Single-Cell Transcriptome Perspective'. *The Journal of Clinical Endocrinology and Metabolism* 102 (6): 2029–38. https://doi.org/10.1210/jc.2016-3524.

Samuelsson, Anne-Maj, Phillippa A. Matthews, Marco Argenton, Michael R. Christie, Josie M. McConnell, Eugene H. J. M. Jansen, Aldert H. Piersma, et al. 2008. 'Diet-Induced Obesity in Female Mice Leads to Offspring Hyperphagia, Adiposity, Hypertension, and Insulin Resistance: A Novel Murine Model of Developmental Programming'. *Hypertension (Dallas, Tex.: 1979)* 51 (2): 383–92. https://doi.org/10.1161/HYPERTENSIONAHA.107.101477.

Sanfins, Alexandra, Patrícia Rodrigues, and David F. Albertini. 2018. 'GDF-9 and BMP-15 Direct the Follicle Symphony'. *Journal of Assisted Reproduction and Genetics* 35 (10): 1741–50. https://doi.org/10.1007/s10815-018-1268-4.

Schmidt, Rebecca L., and Laurel L. Lenz. 2012. 'Distinct Licensing of IL-18 and IL-1β Secretion in Response to NLRP3 Inflammasome Activation'. *PLOS ONE* 7 (9): e45186. https://doi.org/10.1371/journal.pone.0045186.

Shao, Bo-Zong, Zhe-Qi Xu, Bin-Ze Han, Ding-Feng Su, and Chong Liu. 2015. 'NLRP3 Inflammasome and Its Inhibitors: A Review'. *Frontiers in Pharmacology* 6 (November). https://doi.org/10.3389/fphar.2015.00262.

Shen, Hao-Ran, Xiao Xu, and Xue-Lian Li. 2021. 'Berberine Exerts a Protective Effect on Rats with Polycystic Ovary Syndrome by Inhibiting the Inflammatory Response and Cell Apoptosis'. *Reproductive Biology and Endocrinology* 19 (1): 3. https://doi.org/10.1186/s12958-020-00684-y.

Shuvarikov, Andrey A., Michael A. Davis, Katharina Esser-Nobis, and Michael J. Gale. 2018. 'Mitochondrial SLC25 Proteins Interact with NLRP3 to Regulate Inflammasome Function'. *The Journal of Immunology* 200 (1 Supplement): 115.8-115.8.

Smith, Reuben L, Maarten R Soeters, Rob C I Wüst, and Riekelt H Houtkooper. 2018. 'Metabolic Flexibility as an Adaptation to Energy Resources and Requirements in Health and Disease'. *Endocrine Reviews* 39 (4): 489–517. https://doi.org/10.1210/er.2017-00211.

Snider, Alexandria P., and Jennifer R. Wood. 2019. 'Obesity Induces Ovarian Inflammation and Reduces Oocyte Quality'. *Reproduction (Cambridge, England)* 158 (3): R79–90. https://doi.org/10.1530/REP-18-0583.

Stienstra, Rinke, Cees J. Tack, Thirumala-Devi Kanneganti, Leo A. B. Joosten, and Mihai G. Netea. 2012. 'The Inflammasome Puts Obesity in the Danger Zone'. *Cell Metabolism* 15 (1): 10–18. https://doi.org/10.1016/j.cmet.2011.10.011.

Tőzsér, József, and Szilvia Benkő. 2016. 'Natural Compounds as Regulators of NLRP3 Inflammasome-Mediated IL-1β Production'. *Mediators of Inflammation* 2016: 5460302. https://doi.org/10.1155/2016/5460302.

Traba, Javier, and Michael N. Sack. 2017. 'The Role of Caloric Load and Mitochondrial Homeostasis in the Regulation of the NLRP3 Inflammasome'. *Cellular and Molecular Life Sciences: CMLS* 74 (10): 1777–91. https://doi.org/10.1007/s00018-016-2431-7.

Uyar, Asli, Saioa Torrealday, and Emre Seli. 2013. 'Cumulus and Granulosa Cell Markers of Oocyte and Embryo Quality'. *Fertility and Sterility* 99 (4): 979–97. https://doi.org/10.1016/j.fertnstert.2013.01.129.

Wang, F., S. Wang, Z. Zhang, Q. Lin, Y. Liu, Y. Xiao, K. Xiao, and Zhengchao Wang. 2017. 'Activation of NLRP3 Inflammasome in the Ovaries during the Development and Treatment of Polycystic Ovary Syndrome'. *International Journal of Clinical and Experimental Pathology* 10 (January): 5022–30.

Wang, Xiaqiong, Wei Jiang, Yiqing Yan, Tao Gong, Jiahuai Han, Zhigang Tian, and Rongbin Zhou. 2014. 'RNA Viruses Promote Activation of the NLRP3 Inflammasome through a RIP1-RIP3-DRP1 Signaling Pathway'. *Nature Immunology* 15 (12): 1126–33. https://doi.org/10.1038/ni.3015.

Wani, Kaiser, Hind AlHarthi, Amani Alghamdi, Shaun Sabico, and Nasser M. Al-Daghri. 2021. 'Role of NLRP3 Inflammasome Activation in Obesity-Mediated Metabolic Disorders'. *International Journal of Environmental Research and Public Health* 18 (2). https://doi.org/10.3390/ijerph18020511.

Weber, Alexander N. R., Zsófia A. Bittner, Sangeetha Shankar, Xiao Liu, Tzu-Hsuan Chang, Tengchuan Jin, and Ana Tapia-Abellán. 2020. 'Recent Insights into the Regulatory Networks of NLRP3 Inflammasome Activation'. *Journal of Cell Science* 133 (jcs248344). https://doi.org/10.1242/jcs.248344.

Wen, Haitao, Denis Gris, Yu Lei, Sushmita Jha, Lu Zhang, Max Tze-Han Huang, Willie June Brickey, and Jenny P.-Y. Ting. 2011. 'Fatty Acid–Induced NLRP3-ASC Inflammasome Activation Interferes with Insulin Signaling'. *Nature Immunology* 12 (5): 408–15. https://doi.org/10.1038/ni.2022.

Wilding, Martin, Gianfranco Coppola, Brian Dale, and Loredana Di Matteo. 2009. 'Mitochondria and Human Preimplantation Embryo Development'. *Reproduction (Cambridge, England)* 137 (4): 619–24. https://doi.org/10.1530/REP-08-0444.

804 Wolf, Andrea J., Christopher N. Reyes, Wenbin Liang, Courtney Becker, Kenichi Shimada, Matthew
805 L. Wheeler, Hee Cheol Cho, et al. 2016. 'Hexokinase Is an Innate Immune Receptor for the
806 Detection of Bacterial Peptidoglycan'. *Cell* 166 (3): 624–36.
807 https://doi.org/10.1016/j.cell.2016.05.076.
808 Wołodko, Karolina, Juan Castillo-Fernandez, Gavin Kelsey, and António Galvão. 2021. 'Revisiting
809 the Impact of Local Leptin Signaling in Folliculogenesis and Oocyte Maturation in Obese
810 Mothers'. *International Journal of Molecular Sciences* 22 (8).
811 https://doi.org/10.3390/ijms22084270.
812 Wołodko, Karolina, Edyta Walewska, Marek Adamowski, Juan Castillo-Fernandez, Gavin Kelsey,
813 and António Galvão. 2020. 'Leptin Resistance in the Ovary of Obese Mice Is Associated with
814 Profound Changes in the Transcriptome of Cumulus Cells'. *Cellular Physiology and*
815 *Biochemistry: International Journal of Experimental Cellular Physiology, Biochemistry, and*
816 *Pharmacology* 54 (3): 417–37. https://doi.org/10.33594/000000228.
817 Wu, Linda Lin-Yan, Kylie R. Dunning, Xing Yang, Darryl L. Russell, Michelle Lane, Robert J.
818 Norman, and Rebecca L. Robker. 2010. 'High-Fat Diet Causes Lipotoxicity Responses in
819 Cumulus–Oocyte Complexes and Decreased Fertilization Rates'. *Endocrinology* 151 (11):
820 5438–45. https://doi.org/10.1210/en.2010-0551.
821 Yamaguchi, A., O. Hori, D. M. Stern, E. Hartmann, S. Ogawa, and M. Tohyama. 1999. 'Stress-
822 Associated Endoplasmic Reticulum Protein 1 (SERP1)/Ribosome-Associated Membrane
823 Protein 4 (RAMP4) Stabilizes Membrane Proteins during Stress and Facilitates Subsequent
824 Glycosylation'. *The Journal of Cell Biology* 147 (6): 1195–1204.
825 https://doi.org/10.1083/jcb.147.6.1195.
826 Yang, Ching-Chun, Chih-Hsing Wu, Ta-Chun Lin, Yi-Ning Cheng, Chin-Sung Chang, Kuo-Ting
827 Lee, Pei-Jane Tsai, and Yau-Sheng Tsai. 2021. 'Inhibitory Effect of PPARγ on NLRP3
828 Inflammasome Activation'. *Theranostics* 11 (5): 2424–41.
829 https://doi.org/10.7150/thno.46873.
830 Zhang, Tianli, Hiroyasu Tsutsuki, Waliul Islam, Katsuhiko Ono, Kohsuke Takeda, Takaaki Akaike,
831 and Tomohiro Sawa. 2021. 'ATP Exposure Stimulates Glutathione Efflux as a Necessary
832 Switch for NLRP3 Inflammasome Activation'. *Redox Biology* 41 (May): 101930.
833 https://doi.org/10.1016/j.redox.2021.101930.
834 Zhang, Zhenghong, Fan Wang, and Yan Zhang. 2019. 'Expression and Contribution of NLRP3
835 Inflammasome During the Follicular Development Induced by PMSG'. *Frontiers in Cell and*
836 *Developmental Biology* 7. https://doi.org/10.3389/fcell.2019.00256.
837 Zhao, J., and Y. Li. 2012. 'Adenosine Triphosphate Content in Human Unfertilized Oocytes,
838 Undivided Zygotes and Embryos Unsuitable for Transfer or Cryopreservation'. *The Journal*
839 *of International Medical Research* 40 (2): 734–39.
840 https://doi.org/10.1177/147323001204000238.
841 Zhao, Sheng, and Russell D. Fernald. 2005. 'Comprehensive Algorithm for Quantitative Real-Time
842 Polymerase Chain Reaction'. *Journal of Computational Biology: A Journal of Computational*
843 *Molecular Cell Biology* 12 (8): 1047–64. https://doi.org/10.1089/cmb.2005.12.1047.
844 Zhou, Rongbin, Aubry Tardivel, Bernard Thorens, Inpyo Choi, and Jürg Tschopp. 2010.
845 'Thioredoxin-Interacting Protein Links Oxidative Stress to Inflammasome Activation'.
846 *Nature Immunology* 11 (2): 136–40. https://doi.org/10.1038/ni.1831.
847 Zhu, Qifan, and Thirumala-Devi Kanneganti. 2017. 'Cutting Edge: Distinct Regulatory Mechanisms
848 Control Proinflammatory Cytokines IL-18 and IL-1β'. *The Journal of Immunology* 198 (11):
849 4210–15. https://doi.org/10.4049/jimmunol.1700352.

850

Figure Legends

Figure 1. Morphofunctional characterisation of NLRP3 in the ovary of cyclic mice

(A) Experimental design: oestrous cycle synchronisation with eCG and hCG as previously described (Hasegawa et al. 2016). Ovaries were collected from animals in oestrus (E) or dioestrus (D) stage of the cycle. Quantification of mRNA levels of (B) Nod-Like Receptor Protein 3 (*Nlrp3*), caspase-1 (*Casp1*), interleukin-1β (*Il-1β*), interleukin-18 (*Il-18*) by real-time PCR. Abundance of (C) Nod-Like Receptor Protein 3 (NLRP3), (D) pro IL-18 p24, (E) IL-18 p18, (F) pro CASP1 p45 and (G) CASP1 p20 protein during E and D measured by western blotting analysis. Data was normalized to ribosomal protein L37 (*Rpl37*) mRNA expression and β-actin of or glyceraldehyde 3-phosphate dehydrogenase (GAPDH) protein expression. Bars represent mean ± SEM. Statistical analysis between groups was carried out using Mann–Whitney. n=5-7 for real-time PCR analysis and n=6 for immunoblots. Asterisks indicate significant differences (*p< 0.05; **p<0.01). Representative immunohistochemical staining of NLRP3 protein during follicular development in the mouse ovary. Positive staining in brown, counterstaining with heamatoxylin. (H, J) Negative control incubated with secondary antibody. Localisation of NLRP3 in (I) whole ovary of 16 weeks (wk) mice fed chow diet (CD), (K) primary follicles of 16 wk CD mice, (L) secondary follicles of 16 wk high fat diet (HFD) mice, and (M) preantral follicles of 16 wk CD mice. Staining was detected in granulosa and theca cells. Faint staining was observed in the oocytes of all stages of folliculogenesis. Arrows denote granulosa cells, arrow-heads denote theca cells, asterisks denote oocytes. The immunohistochemistry staining was confirmed by immunofluorescent localisation of NLRP3. Positive staining in orange, nuclear counterstaining with DAPI in blue. (N) Negative control 16 wk CD stained with polyclonal rabbit IgG. NLRP3 localised in (O) whole ovary, (P-Q) secondary follicles of 16 wk CD mice, (R-S) preantral follicles of 16 wk HFD mice, (T-U) antral follicles of 16 wk HFD mice. Inserts in top left corners represent magnifications of granulosa cells. Scale bars represent 20 or 100 μm.

Figure 2. Diet induced-obesity changes NLRP3 expression in the ovary

(A) Experimental design: mice were fed either chow diet (CD) or high fat diet (HFD) for 4 weeks (wk) or 16 wk and ovaries were collected during dioestrus stage. Quantification of (B) Nod-Like Receptor Protein 3 (*Nlrp3*), caspase-1 (*Casp1*), interleukin-1β (*Il-1β*), and interleukin-18 (*Il-18*) mRNA by real-time PCR. Abundance of (C) NLRP3, (D) pro CASP1 p45, (E) CASP1 p20, (F) pro

IL-18 p24, (G) IL-18 p18 protein measured by western blotting and (H) IL-1β protein measured by ELISA in ovarian extracts collected from DIO mice. mRNA level was normalized with ribosomal protein L37 (*Rpl37*) value and protein expression with β-actin or glyceraldehyde 3-phosphate dehydrogenase (GAPDH) level. Bars represent mean ± SEM. Differences between control and treatment groups analysed with Mann–Whitney; n=6-9 for real-time PCR analysis, n=8 for immunoblots and n=6 for ELISA. Asterisks indicate significant differences (*p< 0.05; **p<0.01; +p=0.06; +p=0.07 or +p=0.082 – all values indicated).

Figure 3. Leptin signalling in the ovary drive changes of NLRP3 during obesity

A) Experimental design: i) pharmacological hyperleptinemia model, mice were either injected with saline or 100µg of leptin (L) for 16 days ; and ii) genetic obesity model, mice lacking leptin in circulation (*ob/ob* -/-) or control group (*ob/ob* +/?). B) Heatmap illustrating fold of change in expression of mRNA of genes Nod-Like Receptor Protein 3 (*Nlrp3*), caspase-1 (*Casp1*), interleukin-1β (*Il-1β*), interleukin-18 (*Il-18*), apoptosis-associated speck-like protein containing A CARD (*Asc*), interleukin-10 (*Il-10*) and tumour necrosis factor alpha (*Tnf*) in hyperleptinemia and *ob/ob* models determined by real-time PCR. The scale matches colours to log 2 fold change (log2_FC) values. Abundance of (C) NLRP3, (D) pro CASP1 p45, (E) CASP1 p20 measured by wersten blotting and (F) Il-1β quantified by EIA, in the mouse ovarian extracts. Level mRNA normalized with ribosomal protein L37 (*Rpl37*) value and protein expression with β-actin or glyceraldehyde 3-phosphate dehydrogenase (GAPDH) . Bars represent mean ± SEM. Statistical analysis between groups was carried out using Mann–Whitney test. n=6-9 for real-time PCR analysis and n=4-8 for immunoblots. Asterisks indicate significant differences (*p< 0.05; + p=0.07).

Figure 4. Cumulus cells transcriptome analysis from diet- induced obese and pharmacologically hyperleptinemic mice reveals leptin-mediated regulation of NLRP3 inflammasome genes

A) Experimental design: RNA-Seq analysis of differentially expressed genes in cumulus cells collected from mice: i) with diet- induced obesity (DIO) fed chow diet (CD) or high fat diet (HFD) for 4 weeks (wk) or 16 wk ii) with pharmacologically hyperleptinemic (LEPT) injected with saline (C) or 100µg of leptin (L) for 16 days. B) Heatmap illustrating expression of genes from leptin

signalling pathway and NLRP3 inflammasome in LEPT and 4 wk HFD normalized by control group fed CD or injected with saline, respectively. Downregulated genes in blue, upregulated genes in orange. The scale on the right matches colours to log 2 fold change (log2 FC) values. (C) Heatmap showing significant changes in major constitutive genes in both conditions leptin and 4 wk HFD. (D) Five main clusters in the network representing strong interaction between selected genes described in B and genes presented in C. (E) Pie chart that displays the main three gene ontology terms that were significantly enriched in cumulus cells in both conditions LEPT and 4 wk HFD. Gene ontology analysis performed with Gene Ontology Enrichment Analysis and Visualisation Tool. (F) Heatmaps showing conserved genes involved in NLRP3 inflammasome activation, glutathione metabolism and other regulations. log2 FC of reads per million (RPM).

Figure 5. NLRP3 activity in the liver of diet- induced obese, hyperleptinemic and genetically obese mice

(A)Experimental design: i) diet induced obese (DIO) mice were fed chow diet (CD) or high fat diet (HFD) for 4 weeks (wk) or 16 wk; ii) pharmacologically hyperleptinemic mice were treated with saline (C) or 100µg of leptin (L) for 16 days; iii) genetically obese mice lacking leptin (*ob/ob* -/-) and control group (*ob/ob* +/?). (B) Heatmap illustrating fold change in expression of mRNA of genes Nod-Like Receptor Protein 3 (*Nlrp3*), caspase-1 (*Casp1*), interleukin-1β (*Il-1β*), and interleukin-18 (*Il-18*), apoptosis-associated speck-like protein containing a CARD (*Asc*), interleukin-10 (*Il-10*) and tumour necrosis factor alpha (*Tnf*) in DIO, hyperleptinemia and *ob/ob* models in comparison to respective controls, determined by real-time PCR. The scale on the right matches colours to log2 fold change (log2 FC) values. Data normalised to mRNA expression of ribosomal protein L37 (*Rpl37*). Abundance of (C) NLRP3, (D) pro CASP1 p45, (E) CASP1 p20, (F) pro IL-18 p24 in mouse liver of DIO, hyperleptinemic and *ob/ob* mice measured in western blotting analysis. Protein normalised with β-actin or glyceraldehyde 3-phosphate dehydrogenase (GAPDH) level. Bars represent mean ± SEM. Statistical analysis between groups was carried out using Mann–Whitney test; n=6-9 for real-time PCR analysis and n=5-8 for immunoblots. Asterisks indicate significant differences (*p< 0.05; **p<0.01).

Table 1. Specification of antibodies used for Western blotting.

940

Antibody name and specificity	Company, Cat no, RRID no	Antibody dilution
Mouse monoclonal against NLR family pyrin domain containing 3 (NLRP3)	AdipoGen Cat# AG-20B-0014, RRID:AB_2490202	1:1000
Rabbit monoclonal against Caspase 1 (CASP1)	Abcam Cat# ab108362, RRID:AB_10858984	1:1000
Rabbit polyclonal against interleukin-18 (IL-18)	Abcam Cat# ab71495, RRID:AB_1209302	1:250
Mouse monoclonal against β-actin	Sigma-Aldrich Cat# A2228, RRID:AB_476697	1:10 000
Rabbit polyclonal against glyceraldehyde 3-phosphate dehydrogenase (GAPDH)	Abcam Cat# ab9485, RRID:AB_307275	1:2500
Goat anti-Mouse IgG (H+L) Secondary Antibody, HRP	Thermo Fisher Scientific Cat# 31430, RRID:AB_228307	1:1000
Goat anti-Rabbit IgG (H+L) Secondary Antibody, HRP	Thermo Fisher Scientific Cat# 31460, RRID:AB_228341	1:20 000
Goat anti-Mouse IgG (H+L) Secondary Antibody, AP	Thermo Fisher Scientific Cat# 31321, RRID:AB_10959407	1:1000
Goat Anti-Rabbit IgG (whole molecule) Secondary Antibody, AP	Sigma-Aldrich Cat# A3687, RRID:AB_258103	1:10 000

941

942

943

944

945

946

947

948

949

950

951

952

953

Gene name	Gene symbol	GenBank Accession no.	Sequences 5'-3'	Length (base pairs)

954

955

956

957

958

959

960

961

962 **Table 2.** Specific primers used for quantitative real-time PCR.

963

964

965

NLR family pyrin domain containing 3	*Nlrp3*	NM_145827.4	F: TGGATGGGTTTGCTGGGATA R: TGCTTGGATGCTCCTTGACC	190
Caspase 1	*Casp1*	NM_009807.2	F: CATGCCGTGGAGAGAAACAA R: GGTGTTGAAGAGCAGAAAGCAA	151
Interleukin-1β	*IL-1β*	NM_008361.4	F: TTGACGGACCCCAAAAGATG R: GCTTCTCCACAGCCACAATGA	144
Interleukin-18	*Il-18*	NM_008360.2	F: GAAGAAAATGGAGACCTGGAATCA R: TCTGGGGTTCACTGGCACTT	157
Apoptosis-Associated Speck-Like Protein Containing A CARD	*Asc*	NM_023258.4	F: GCTTAGAGACATGGGCTTACAGGA R: CCAGCACTCCGTCCACTTCT	179
Interleukin-10	*Il-10*	NM_010548.2	F: CCTGGGTGAGAAGCTGAAGAC R: CTGCTCCACTGCCTTGCTCT	91
Tumor necrosis factor	*Tnf*	NM_001278601.1	F: GCCACCACGCTCTTCTGTCT R: TGAGGGTCTGGGCCATAGAA	106
Ribosomal protein L37	*Rpl37*	NM_026069.3	F:CTGGTCGGATGAGGCACCTA R: AAGAACTGGATGCTGCGACA	108

966

967 **Table 3.** Body weight measurement of 3 mouse models

968 Diet induced obese (DIO) mice were fed chow diet (CD) or high fat diet (HFD); ii)
969 pharmacologically hyperleptinemic mice were treated with saline (C) or leptin (L) for 16 days; iii)
970 genetically obese mice lacking leptin (*ob/ob* -/-) and control group (*ob/ob* +/?). Statistical analysis
971 between groups was carried out using T-test. Asterisks indicate significant differences (**p< 0.01;
972 ***p< 0.001; ****p<0.0001).

973

974

	0 wk	**4 wk**	**8 wk**	**12 wk**	**16 wk**
CD	17.0 (±0.6)	19.7 (±1.0)	20.0 (±0.9)	20.9 (±1.0)	22.6 (±2.5)
HFD	19.4 (±0.8)	24.8 (±2.5)****	29.1 (±3.6)****	33.1 (±4.3)****	37.6 (±3.7)****
	0 d	**3 d**	**9 d**	**12 d**	**16 d**
C	21.7 (±1.7)	22.8 (±2.0)	22.1 (±2.1)	21.5 (±1.6)	21.9 (±1.9)
L	21.8 (±1.9)	20.5 (±1.9)	19.0 (±1.4)**	18.5 (±1.2)***	19.4 (±1.7)
	8 wk	**9 wk**	**10 wk**	**11 wk**	**12 wk**
ob/ob +/?	20.9 (±1.6)	21.5 (±1.6)	22.2 (±1.6)	22.8 (±2.1)	22.7 (±2.1)
ob/ob -/-	39.8 (±5.4)****	43.1 (±5.0)****	45.0 (±4.7)****	47.4 (±5.7)****	48.8 (±4.0)****

975

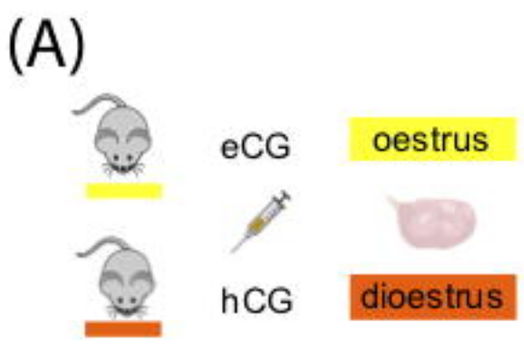

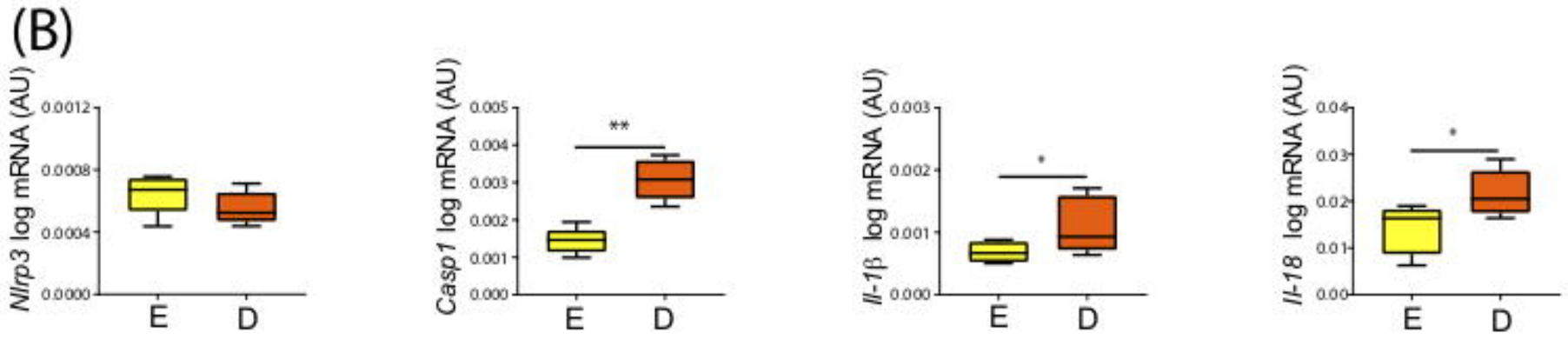

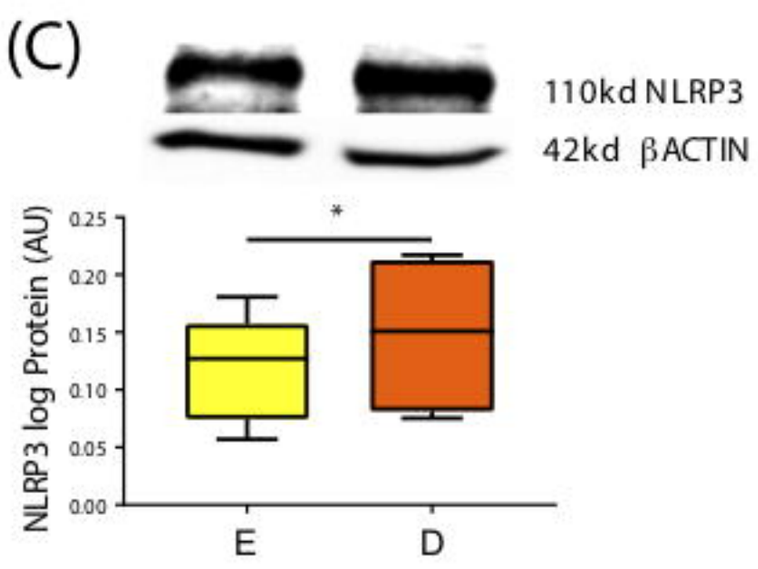

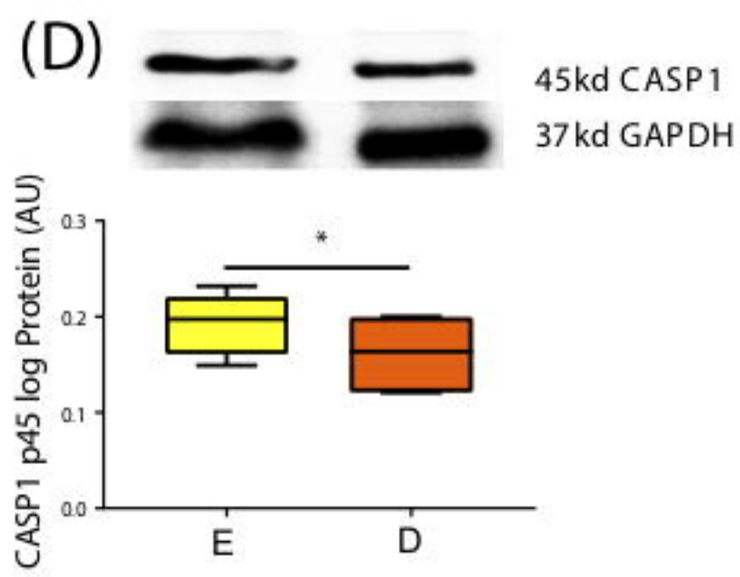

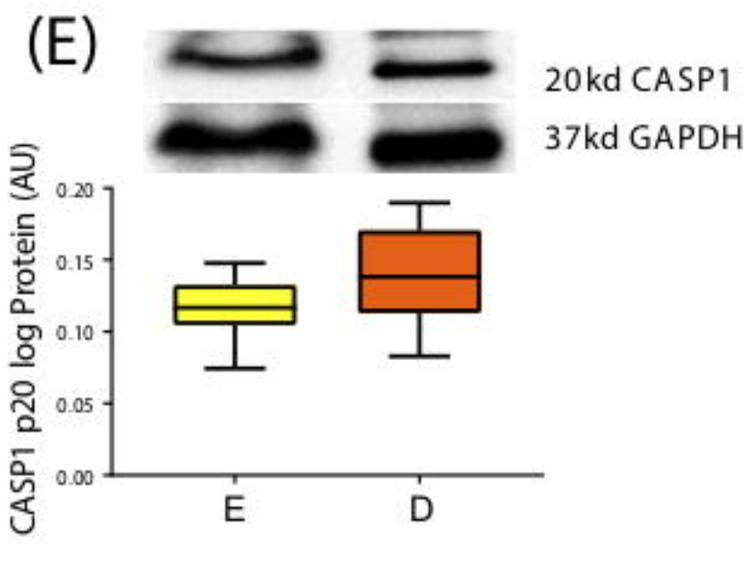

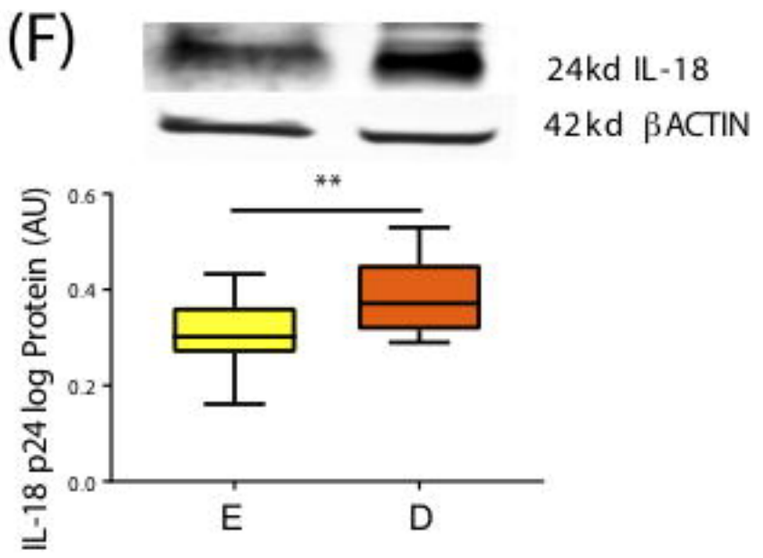

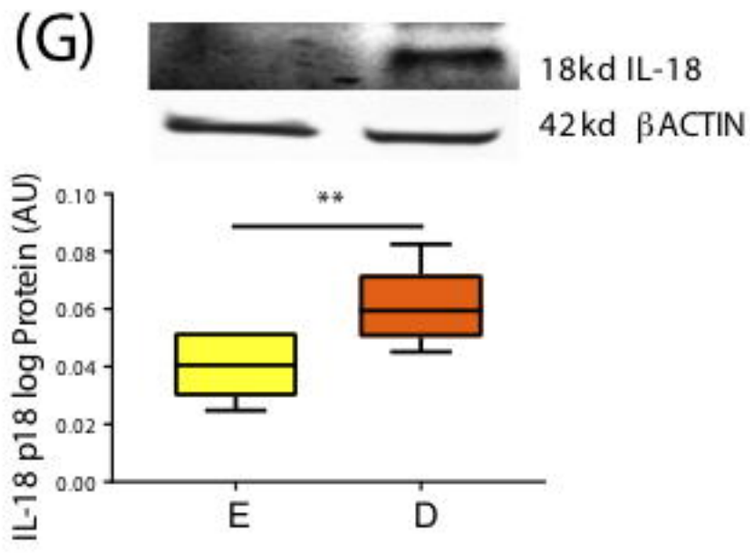

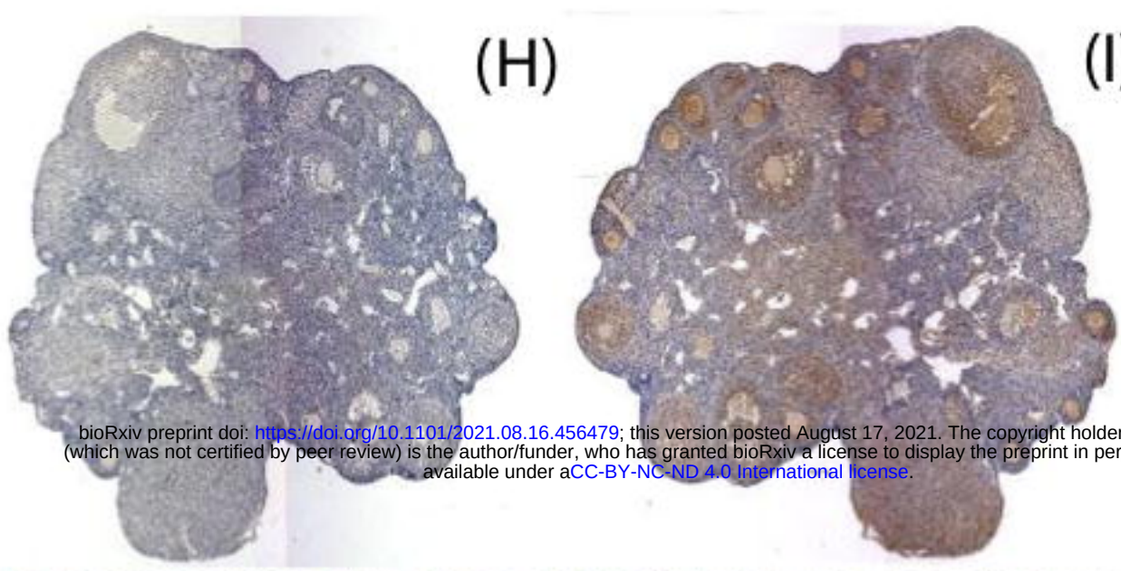

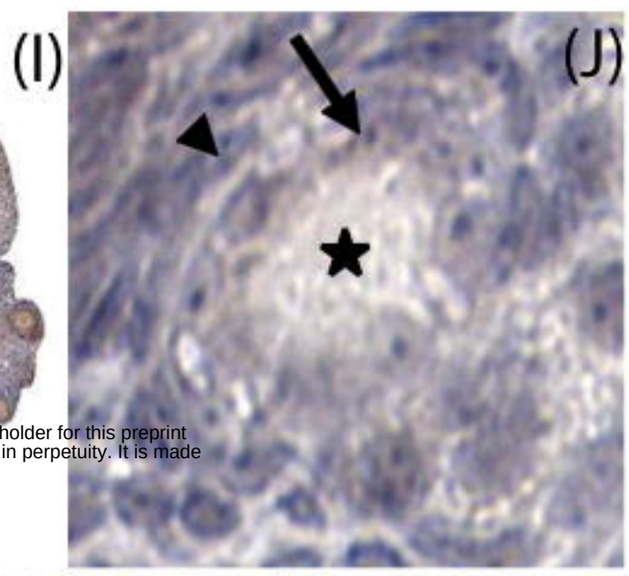

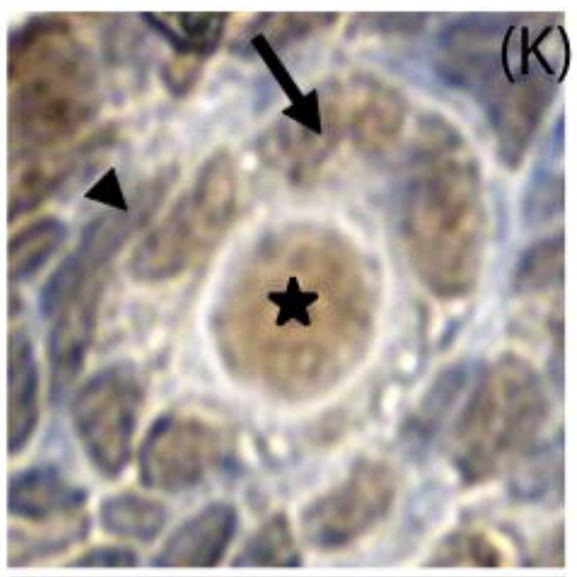

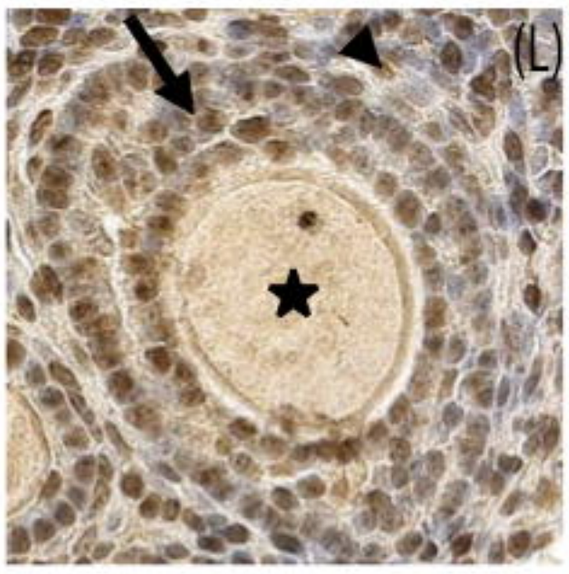

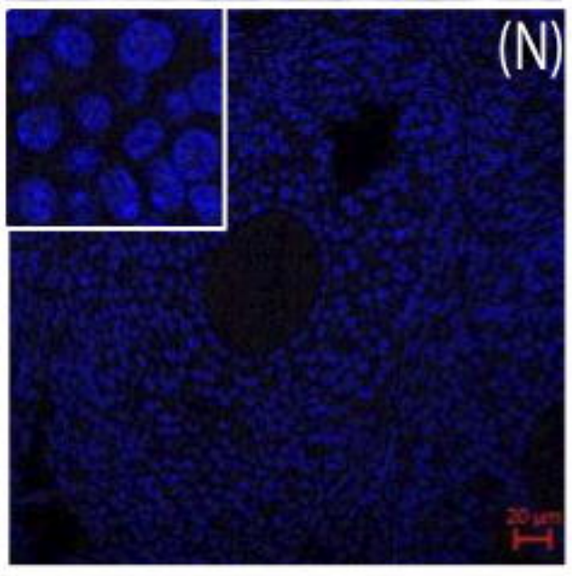

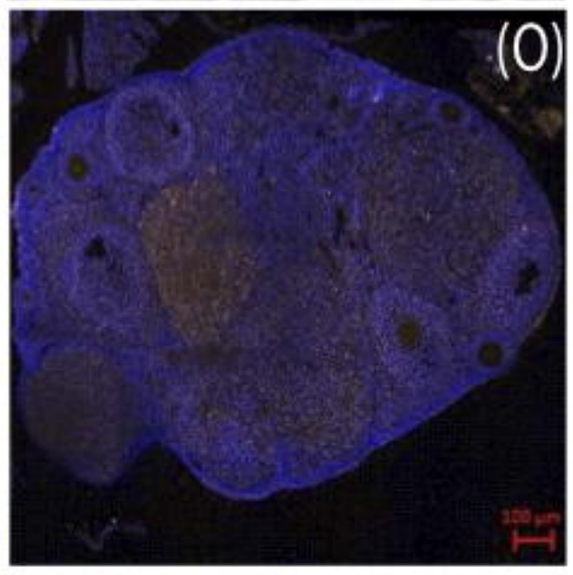

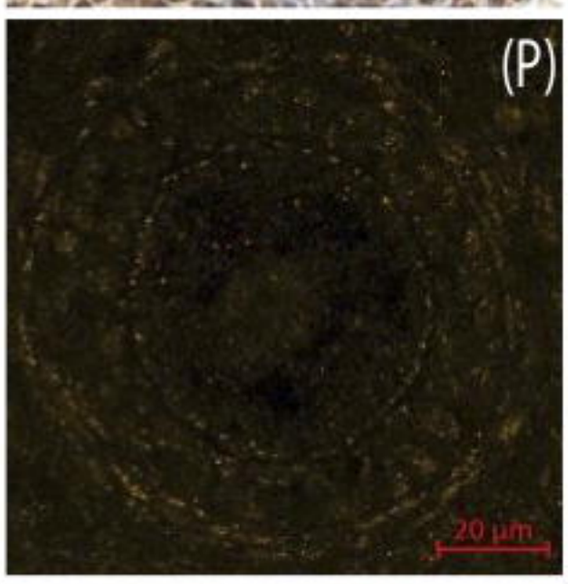

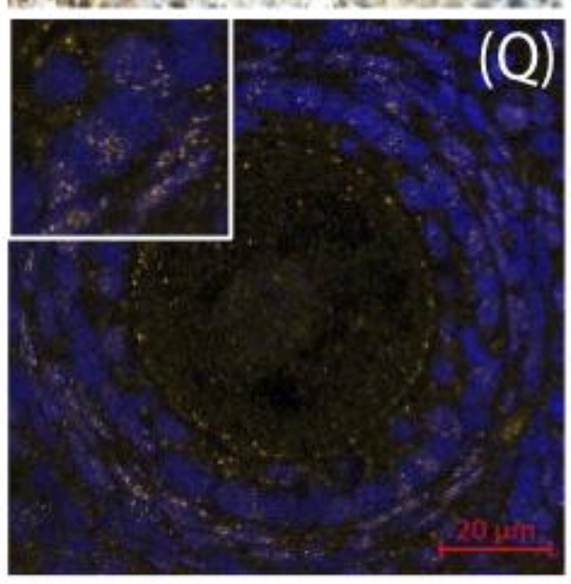

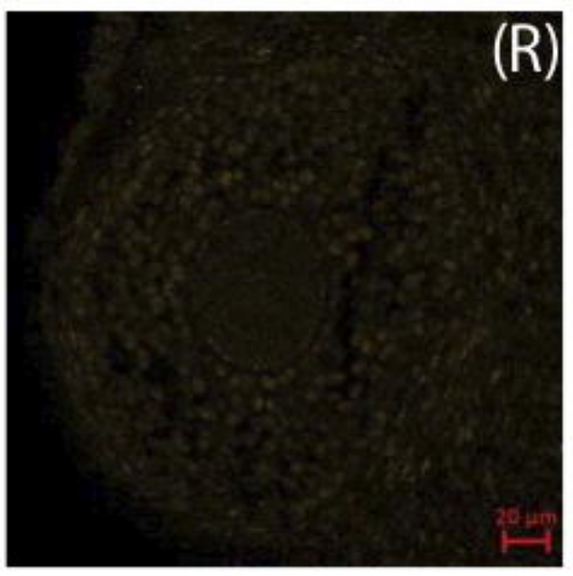

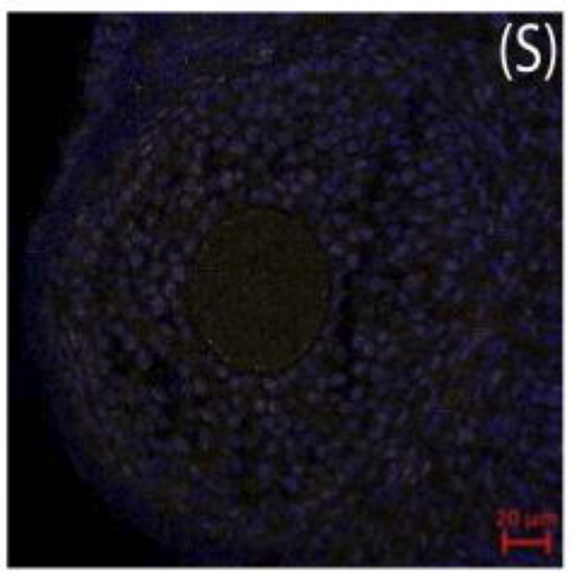

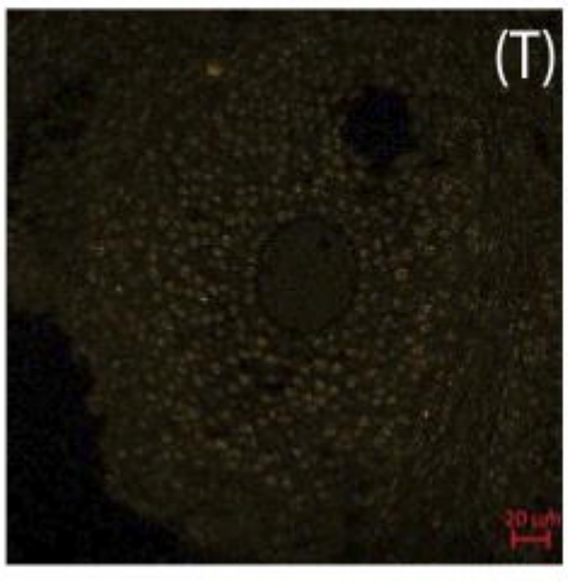

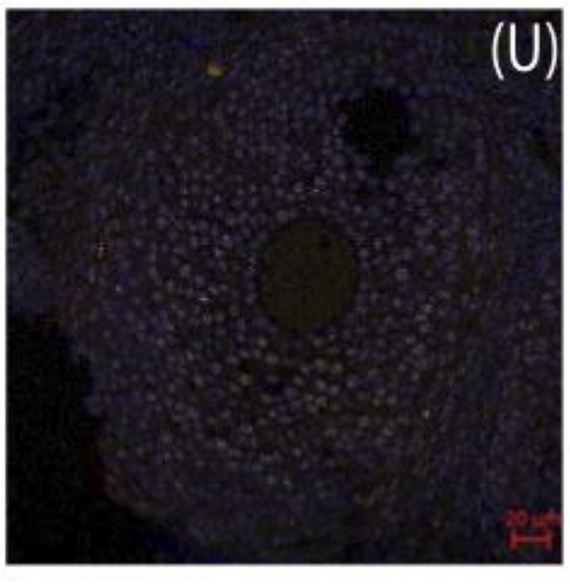

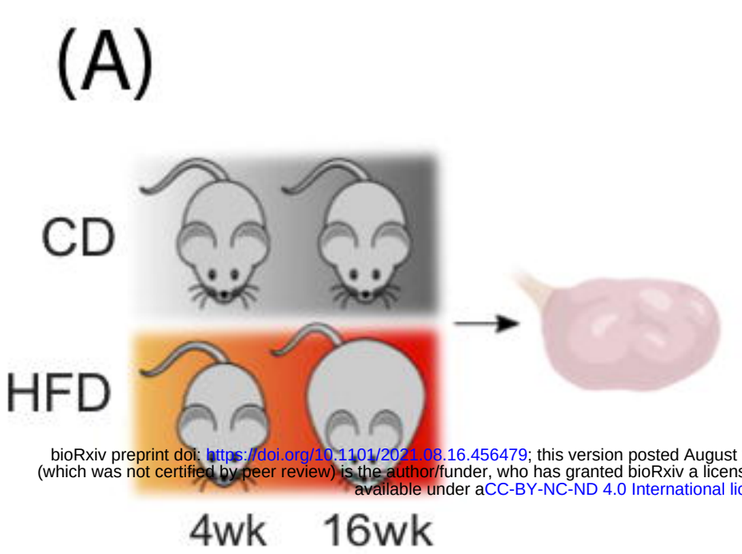

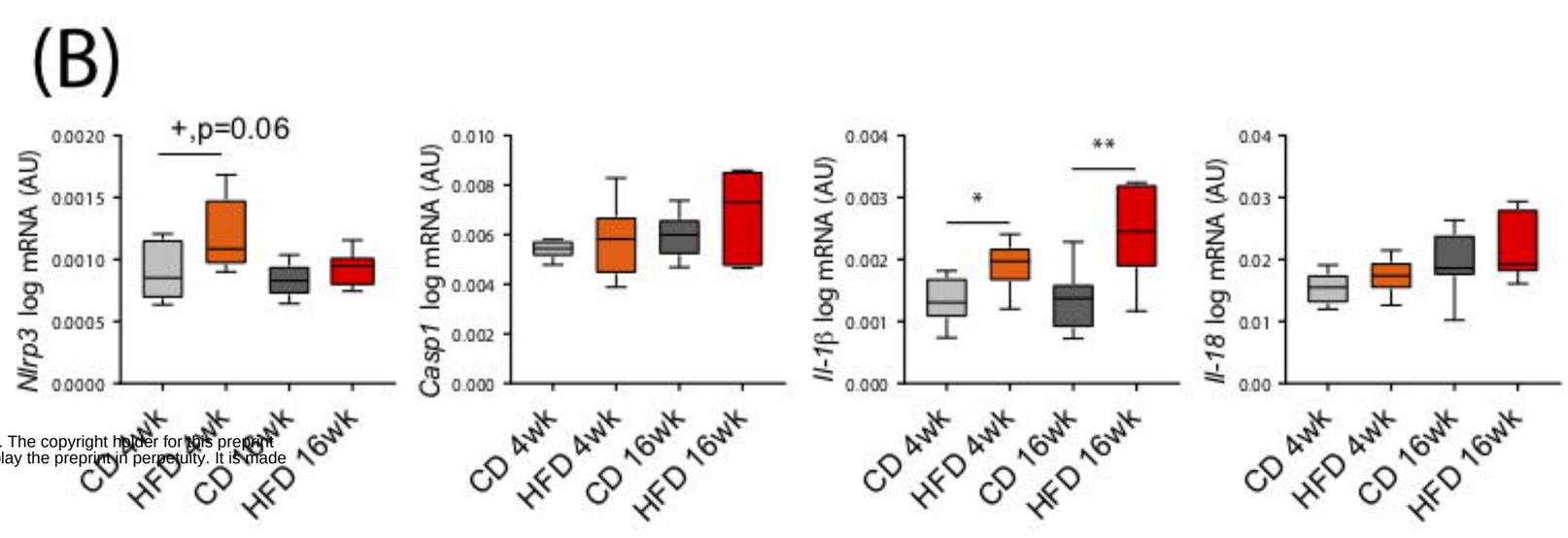

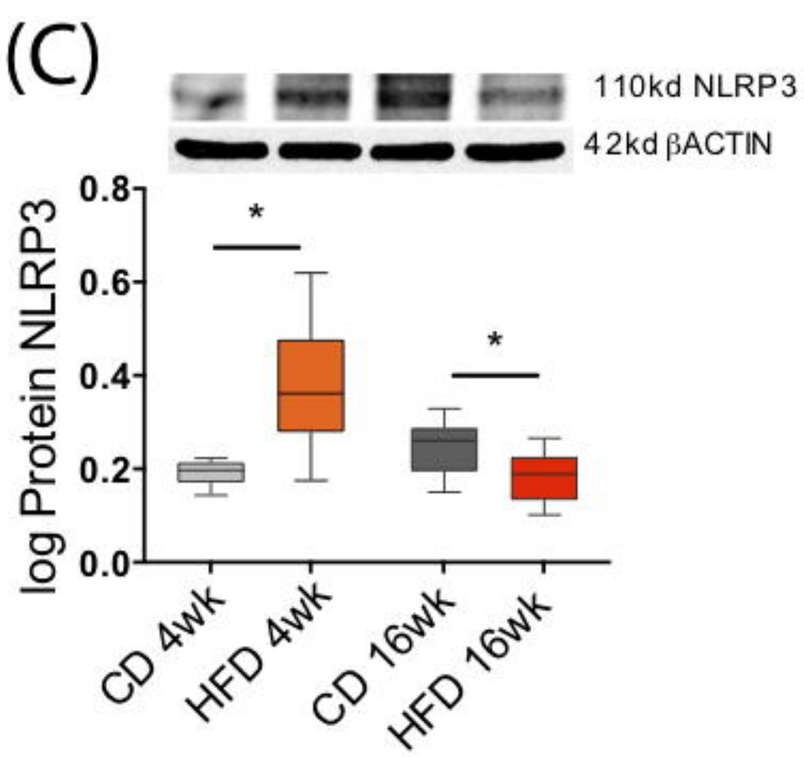

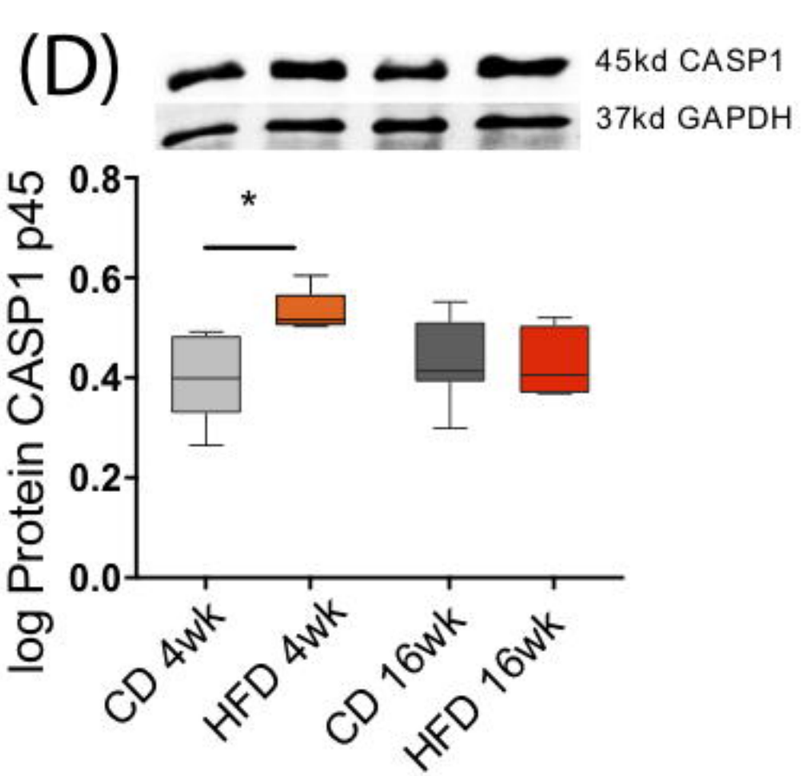

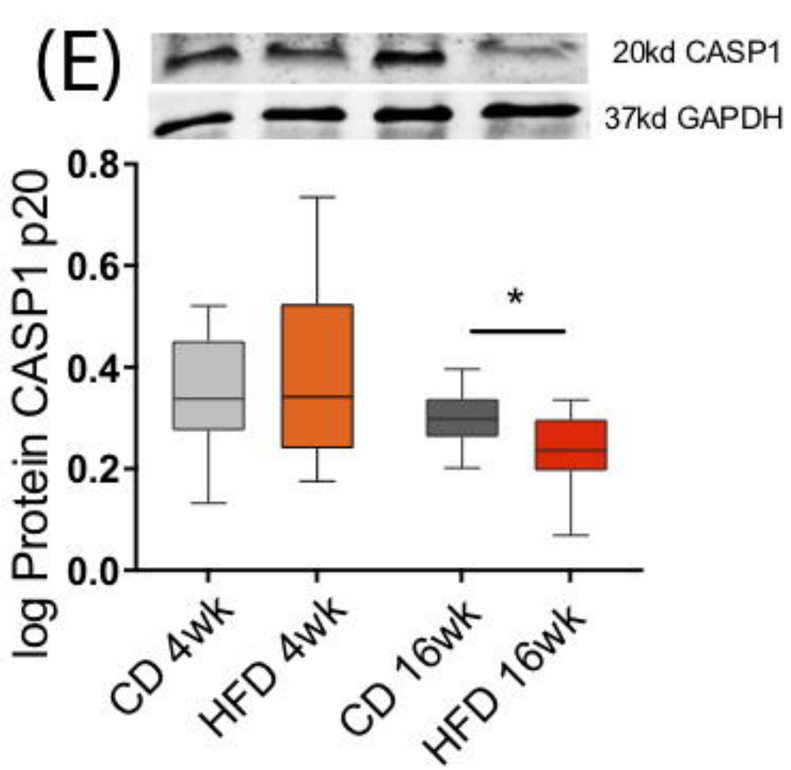

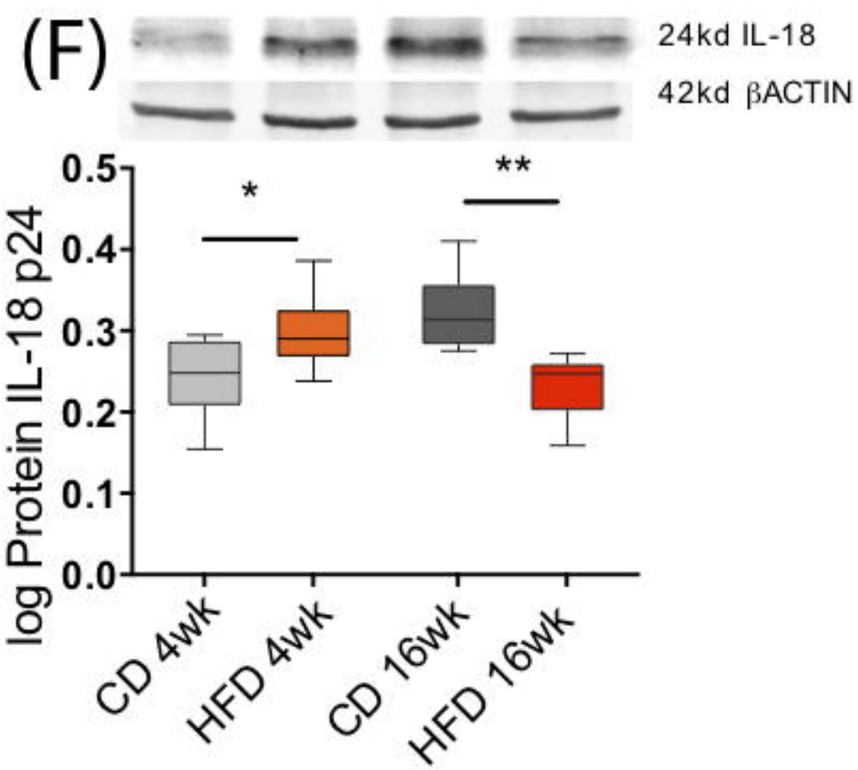

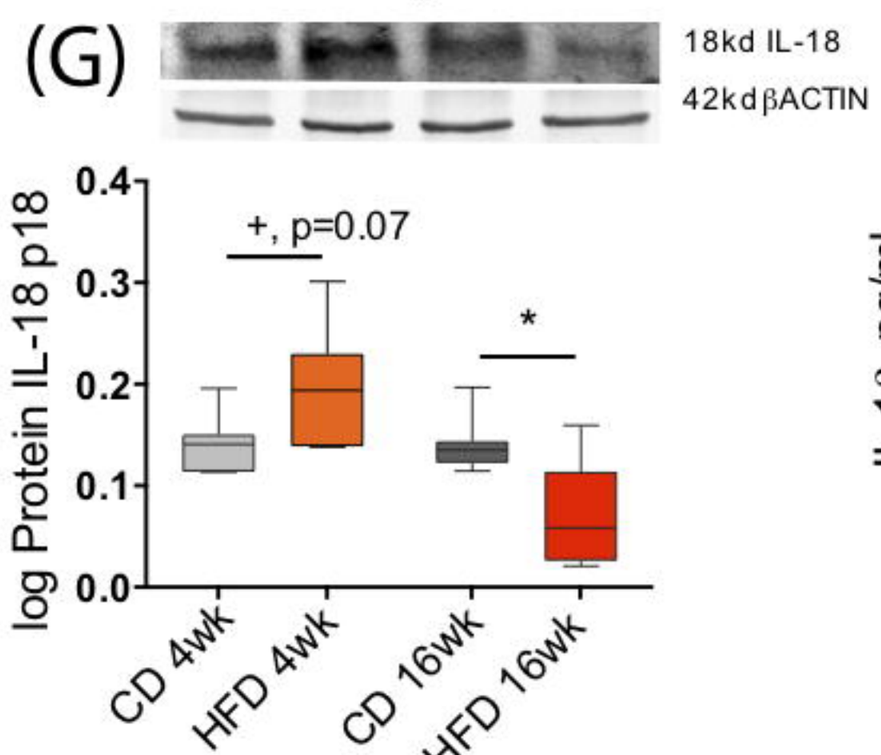

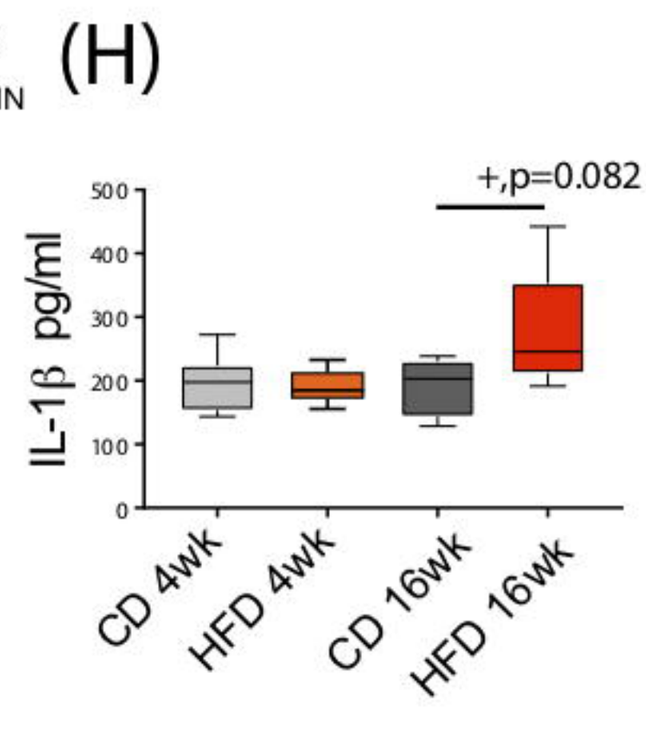

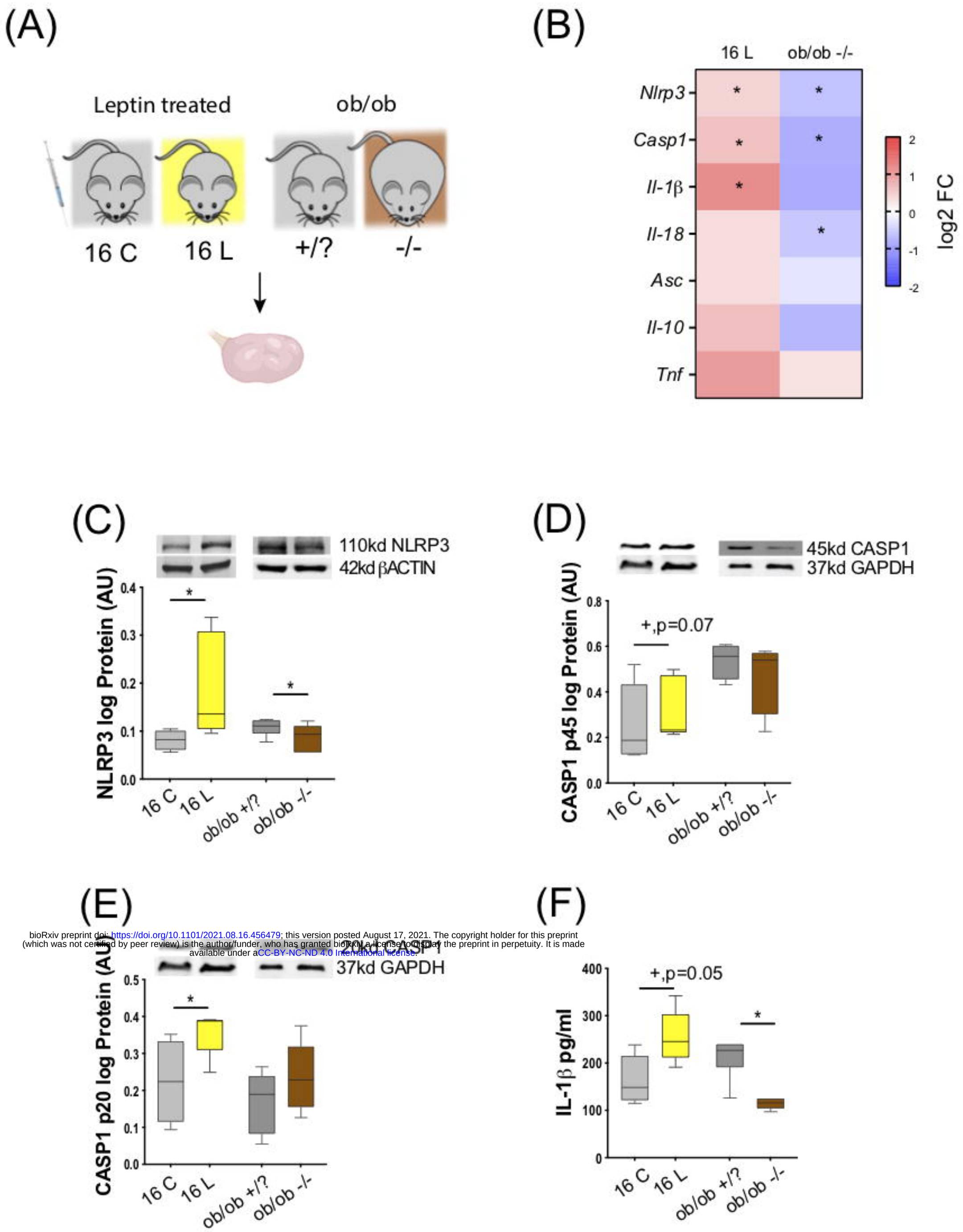

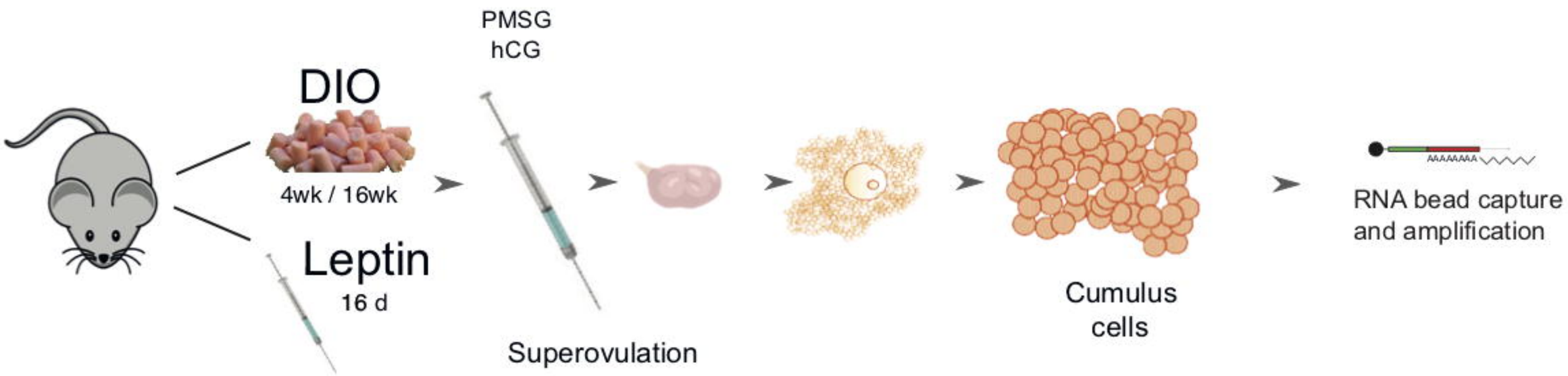

(A)

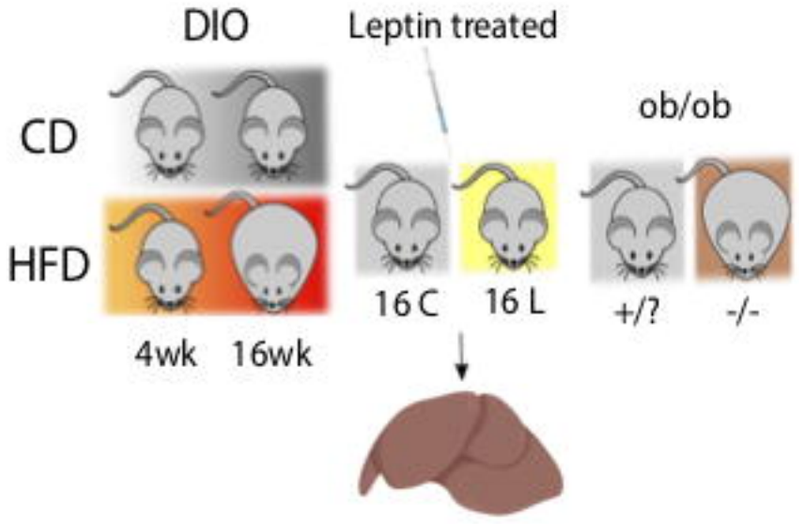

(B)

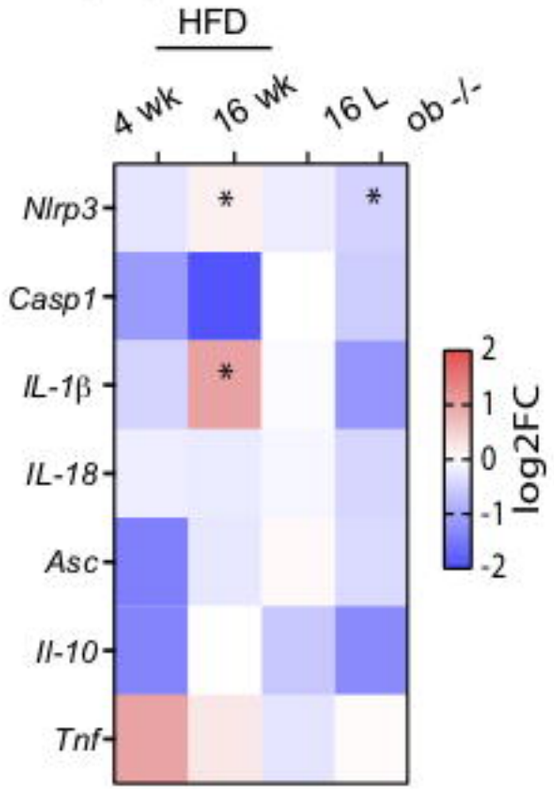

(C)

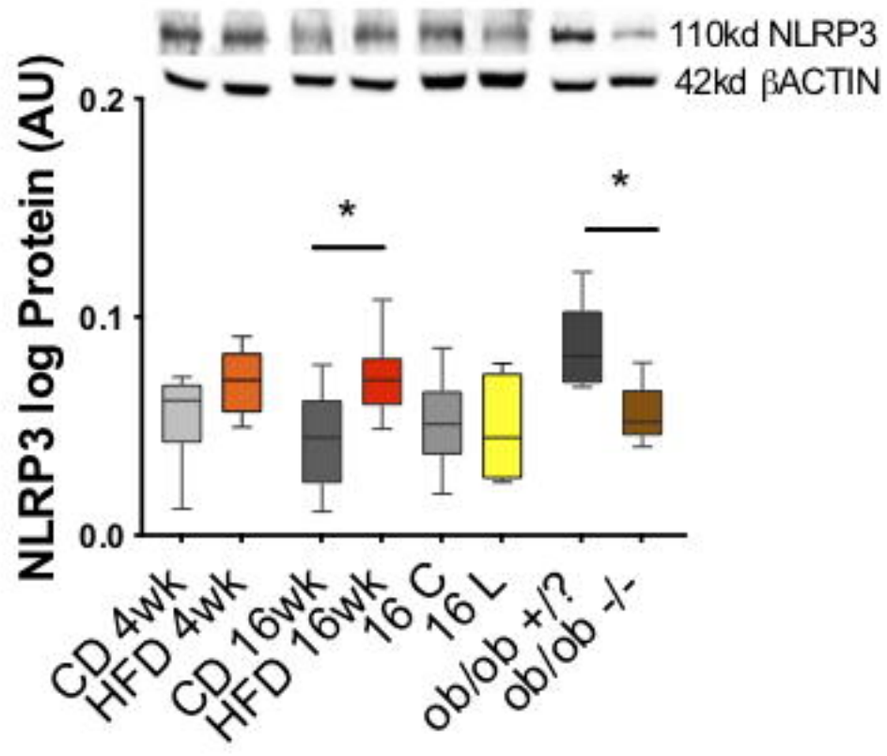

(D)

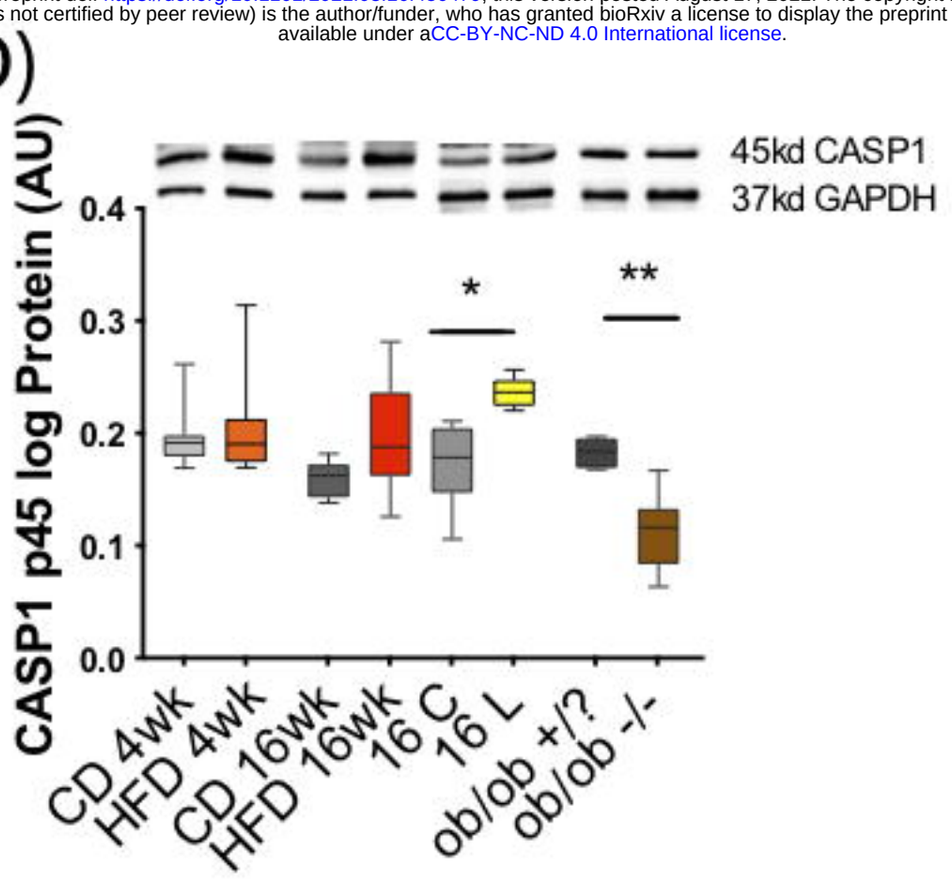

(E)

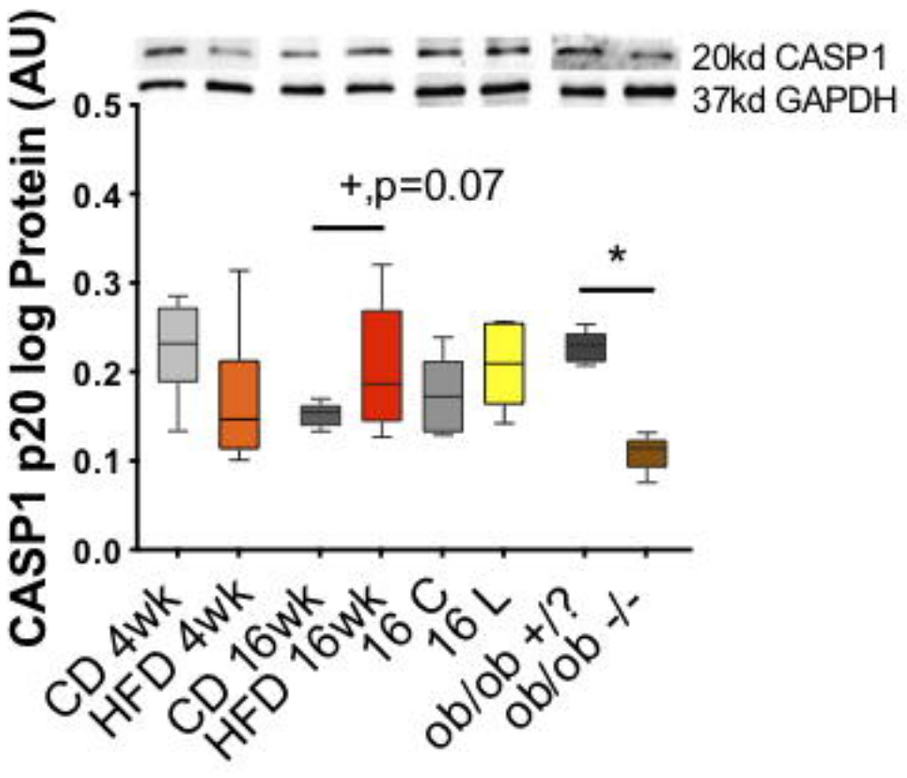

(F)

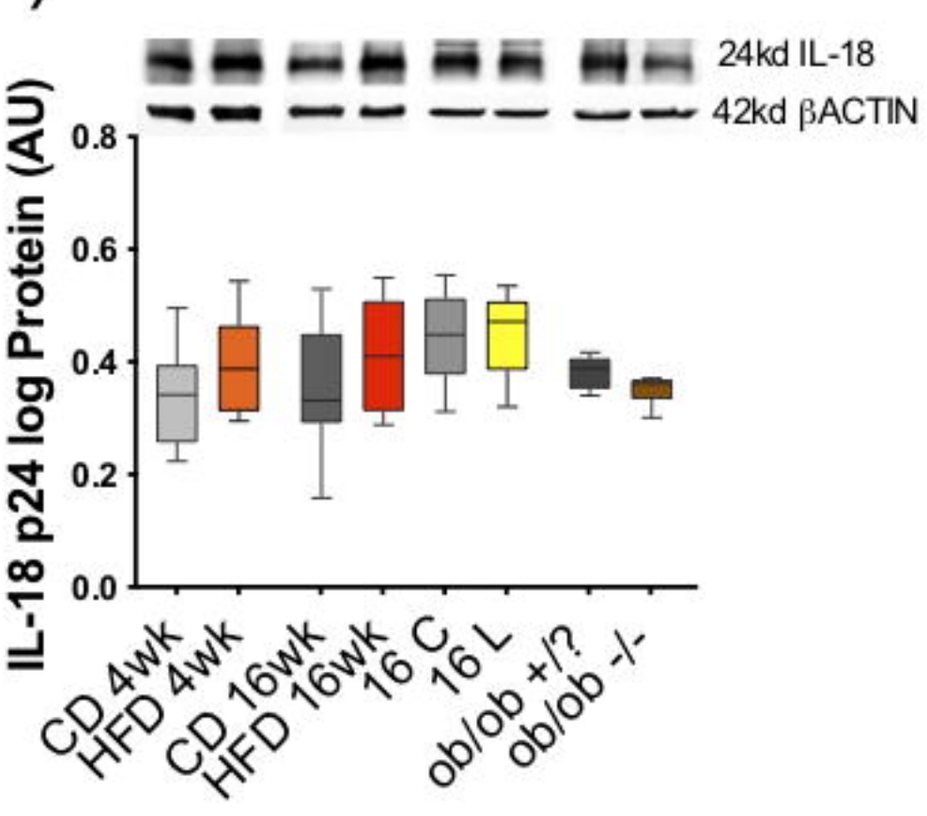

(G)